

3048
RECEIVED BY DTE DEC 2 1968


SC-CR-68-3730
August 1968

CONTRACT REPORT

MASTER

CALIBRATION OF A KERR CELL SYSTEM
FOR HIGH VOLTAGE PULSE MEASUREMENTS

Prepared by
Esther C. Cassidy
H. N. Cones
National Bureau of Standards

SANDIA LABORATORIES 

OPERATED FOR THE U. S. ATOMIC ENERGY COMMISSION BY SANDIA CORPORATION | ALBUQUERQUE, NEW MEXICO; LIVERMORE, CALIFORNIA

DISTRIBUTION OF THIS DOCUMENT IS UNLIMITED

DISCLAIMER

This report was prepared as an account of work sponsored by an agency of the United States Government. Neither the United States Government nor any agency Thereof, nor any of their employees, makes any warranty, express or implied, or assumes any legal liability or responsibility for the accuracy, completeness, or usefulness of any information, apparatus, product, or process disclosed, or represents that its use would not infringe privately owned rights. Reference herein to any specific commercial product, process, or service by trade name, trademark, manufacturer, or otherwise does not necessarily constitute or imply its endorsement, recommendation, or favoring by the United States Government or any agency thereof. The views and opinions of authors expressed herein do not necessarily state or reflect those of the United States Government or any agency thereof.

DISCLAIMER

Portions of this document may be illegible in electronic image products. Images are produced from the best available original document.

Issued by Sandia Corporation,
a prime contractor to the
United States Atomic Energy Commission

LEGAL NOTICE

This report was prepared as an account of Government sponsored work. Neither the United States, nor the Commission, nor any person acting on behalf of the Commission:

A. Makes any warranty or representation, expressed or implied, with respect to the accuracy, completeness, or usefulness of the information contained in this report, or that the use of any information, apparatus, method, or process disclosed in this report may not infringe privately owned rights; or

B. Assumes any liabilities with respect to the use of, or for damages resulting from the use of any information, apparatus, method, or process disclosed in this report.

As used in the above, "person acting on behalf of the Commission" includes any employee or contractor of the Commission, or employee of such contractor, to the extent that such employee or contractor of the Commission, or employee of such contractor prepares, disseminates, or provides access to, any information pursuant to his employment or contract with the Commission, or his employment with such contractor.

SC-CR-68-3730

CALIBRATION OF A KERR CELL SYSTEM
FOR HIGH VOLTAGE PULSE MEASUREMENTS

FINAL REPORT

August 1968

Prepared by

Esther C. Cassidy and H. N. Cones
National Bureau of Standards
Boulder, Colorado

for

Sandia Laboratories

under

Contract No. ASB28-8572

LEGAL NOTICE

This report was prepared as an account of Government sponsored work. Neither the United States, nor the Commission, nor any person acting on behalf of the Commission:

A. Makes any warranty or representation, expressed or implied, with respect to the accuracy, completeness, or usefulness of the information contained in this report, or that the use of any information, apparatus, method, or process disclosed in this report may not infringe privately owned rights; or

B. Assumes any liabilities with respect to the use of, or for damages resulting from the use of any information, apparatus, method, or process disclosed in this report.

As used in the above, "person acting on behalf of the Commission" includes any employee or contractor of the Commission, or employee of such contractor, to the extent that such employee or contractor of the Commission, or employee of such contractor prepares, disseminates, or provides access to, any information pursuant to his employment or contract with the Commission, or his employment with such contractor.

DISTRIBUTION OF THIS DOCUMENT IS UNLIMITED

TABLE OF CONTENTS

	<u>Page</u>
I. INTRODUCTION	7
II. THE KERR CELL DESIGN AND LIQUID	8
III. ELECTRICAL INSTRUMENTATION AND PROCEDURE	18
IV. CALIBRATION WITH A UNIFORM FIELD	27
A. Pulse Divider Techniques	29
B. Two-Pulse Technique	29
C. Detection and Measurement of Bias at Minimum	31
V. THE NONUNIFORM ELECTRIC FIELD	33
VI. CALIBRATION WITH A NONUNIFORM FIELD DISTRIBUTION	41
A. Pulse Divider Technique	41
B. Calibration from Measurements of Direct Voltages which Produce Minimum Transmission	41
C. "Beam Expander Method"	45
VII. SUMMARY AND CONCLUSION	49
VIII. FUTURE PLANS	49
IX. ACKNOWLEDGMENTS	50
X. REFERENCES	50

LIST OF ILLUSTRATIONS

<u>Figure</u>	<u>Page</u>
1. Kerr Cell No. 1 (interelectrode distance ≈ 0.75 cm) installed in micrometer-driven, spring-loaded holder.	9
2. Time-resolved measurements of voltage (V) and current (i) before and after purification of nitrobenzene.	11
3. Apparatus used for purification of nitrobenzene and filling of Kerr cell.	13
4. Glass to polyethylene seal used in purification and cell-filling system.	14
5. The chromatographic adsorption column after passage and purification of nitrobenzene.	14
6. Circuit used for determination of resistance of Kerr cell.	16
7. The electrical triggering, delay, and measuring instrumentation.	19
8. Voltage divider and Kerr cell measurements of a 20 kV pulse.	20
9. Calibrated voltage divider (top) and Kerr cell measurements of peak amplitude of a high voltage pulse.	22
10. Layout of optical system.	23
11. Relative transmitted light intensity vs. relative field strength with numerical values assigned to successive transmission maxima and minima.	25
12. Superimposed pulse divider (top traces in each record) and Kerr system (bottom traces) measurements.	28
13. Laser photographs showing profile of electric field in Kerr cell.	35
14. Profile of the electric field distribution over the inter-electrode area of Cell No. 1 ($d \approx 0.75$ cm).	36

LIST OF ILLUSTRATIONS (Cont.)

<u>Figure</u>		<u>Page</u>
15.	Relative intensity of transmitted beam as a function of distance between the electrodes of Cell No. 1 as recorded by photomultiplier tube, at various applied voltages: $V_1 = 13,097$, $V_2 = 14,640$, $V_3 = 15,160$, $V_4 = 16,045$, $V_5 = 17,082$, and $V_6 = 18,086$ volts.	38
16.	Relative field strength in Cell No. 1 as a function of inter-electrode distance, as derived from the photomultiplier records of I/I_m and n in Fig. 15.	39
17.	Measurements of the direct voltages V_{min} which produced the first transmission minimum along various paths between the electrodes of Cell No. 1	40
18.	Relative electric field strength (E/E_{min}) as a function of interelectrode distance in Cell No. 1 as deduced from the measurements of Fig. 17.	44
19.	Setup used for "Beam Expander Calibration" of Kerr cells.	46

LIST OF TABLES

	<u>Page</u>
Table 1. Calibrations of a Kerr Cell with Near-Uniform Electric Field Distribution	32
Table 2. Calibrations of a Cell (No. 1) with Nonuniform Electric Field Distribution	42
Table 3. Calibrations of Cells with Nonuniform Electric Field Distributions	47
Table 4. Pulse Measurement Experiments	48

NOTATION

The following symbols, which are used repeatedly in the text, are collected and defined for the convenience of the reader.

- v_D = calibrated divider measurement of an applied pulse voltage.
- v_K = Kerr system measurement of an applied pulse voltage.
- I = the instantaneous intensity of the beam transmitted by a given Kerr system upon application of voltage to the Kerr cell.
- I_m = the maximum intensity transmitted by the system.
- E = the instantaneous electric field intensity imposed by application of voltage across the plates of the Kerr cell.
- E_m = the field intensity which produces the first transmission maximum I_m in a given cell.
- E_{min} = the field intensity which produces the first transmission minimum.
- $(E_m d)$ = the Kerr cell constant, i.e., the voltage which produces the first transmission maximum I_m when the electric field distribution is uniform.
- d = the Kerr cell interelectrode distance.
- V_{min} = the voltage which produces the first transmission minimum I_{min} . When the field is uniform, $V_{min} = \sqrt{2}(E_m d)$; when the field is nonuniform, V_{min} is a function of light path (e.g., see Fig. 17).
- V_{BIAS} = the direct bias voltage applied to the cell.

CALIBRATION OF A KERR CELL SYSTEM FOR HIGH VOLTAGE PULSE MEASUREMENTS

I. INTRODUCTION

Many normally optically isotropic liquids exhibit birefringence when subjected to an electrostatic field. When polarized light is passed between two electrodes immersed in a vessel containing such a liquid, application of a high voltage alters the state of polarization of the light. If the vessel is installed between "crossed" polarizers, the applied voltage in effect causes modulation or gating of the light. Devices (Kerr cells) utilizing this phenomenon, the so-called Kerr electro-optical effect [1], are often used as ultra high-speed optical shutters and laser "Q-switches".

The Kerr cell has also been used for measurement of high voltages, with its application for this purpose being reported as early as 1930 [2]. In 1956, Namba [3] utilized the similar Pockels effect for measurements of direct voltages up to 10 kV. In 1963, Ettinger and Venezia [4] developed a pulse measuring system based on the Kerr effect. More recently, a much improved system for measurement of pulses between 30 and 100 kV was described by Wunsch and Erteza [5]. These systems, particularly the latter, offer unique advantages over more conventional resistive and/or capacitive divider techniques of high-voltage pulse measurements, including the following: (1) measurement resolution increases with the magnitude of the applied voltage; (2) the system has a linear frequency response to about 100 MHz; and (3) the measuring circuit is electrically isolated from the main high-voltage circuit, thus avoiding sources of error [6] which are characteristic of divider techniques.

To date, most pulse voltage measurements are made by use of calibrated resistive or capacitive dividers [7]. Calibration is achieved either by low voltage measurements (and extrapolation to high voltages), or by comparison at high voltage with a "standard" divider (calibrated at low voltages). The dividing ratio at higher voltages is therefore always somewhat uncertain. The present work reports development and evaluation of several methods for calibrating a Kerr cell system, similar to that described in reference [5], for measurement of pulses with peak amplitudes as high as 100 kV. Techniques which permit calibration without reference to calibrated divider measurements are emphasized, inasmuch as they provide an independent check of divider methods, thus adding considerably to our confidence in the accuracy of high voltage pulse measurements.

Indeed, it now appears that measurements accurate to within $\pm 0.5\%$ of pulses considerably in excess of 100 kV are feasible with the Kerr cell technique. With further refinements, its use as a "standard" for calibration of pulse dividers is anticipated.

II. THE KERR CELL DESIGN AND LIQUID

Since Kerr cells suitable for high voltage pulse measurements are not commercially available and since calibration techniques depend upon cell construction and the purity of its liquid, some discussion of these aspects is required. The cells used in the present work are similar in design to those described by Zarem *et al* [8]. Glass to Kovar seals are used for insertion of the electrodes (parallel nickel plates) into the cell which is filled with high-purity nitrobenzene. One cell, with 0.2 cm x 1.5 cm x 10 cm long electrodes and an interplate distance of about 0.25 cm was used for measurements of pulses with peak amplitudes of up to 10 kV. Two other cells, one with plate dimensions 0.2 cm x 1.5 cm x 7.5 cm (referred to as Cell No. 1 in the text--see Fig. 1) and the other with plate dimensions 0.2 cm x 1.5 cm x 10 cm (Cell No. 2), were constructed with an interelectrode distance of about 0.75 cm. Although

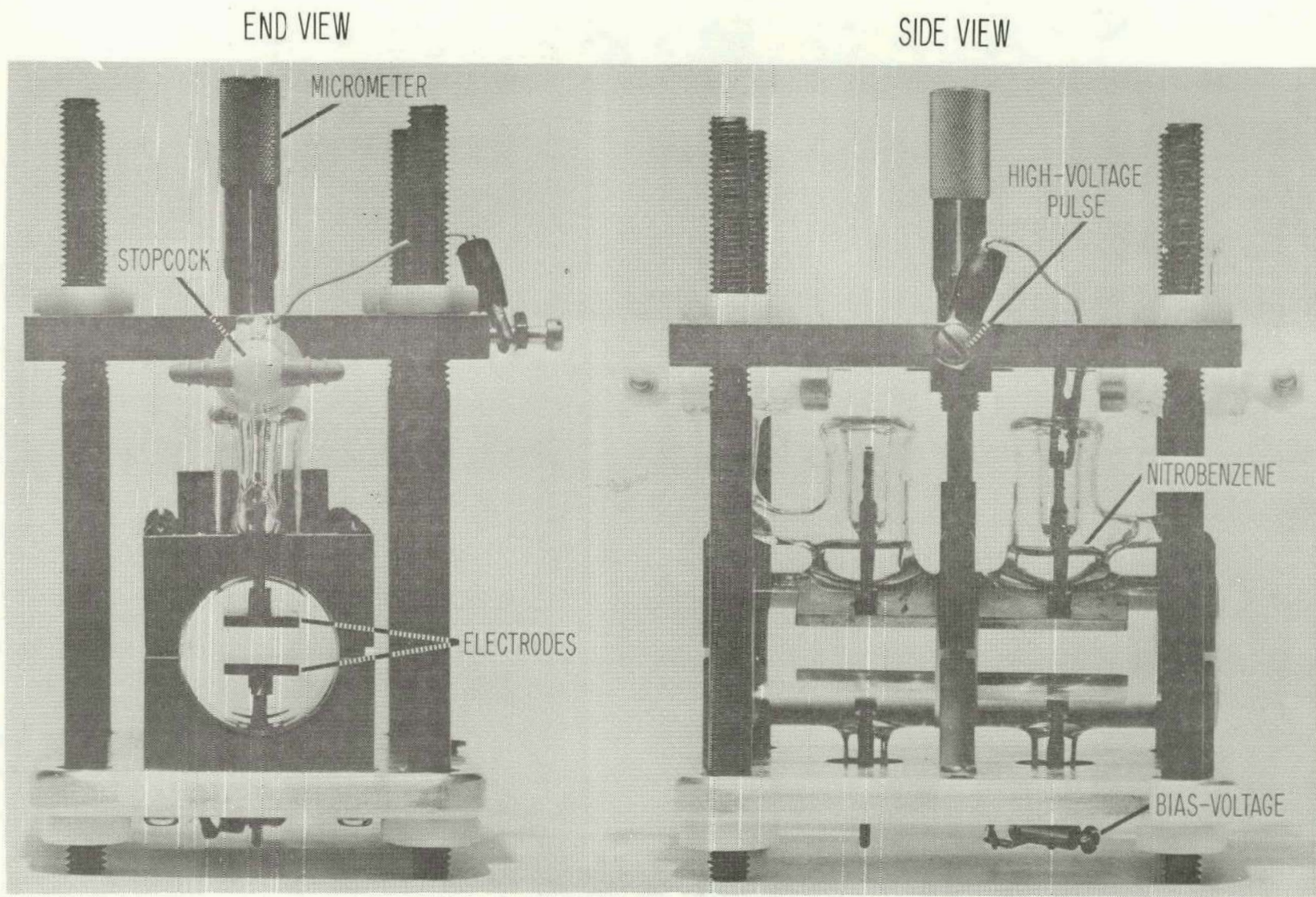


Fig. 1. Kerr Cell No. 1 (interelectrode distance ≈ 0.75 cm) installed in micrometer-driven, spring loaded holder.

the latter cells were designed for use with voltages as high as 60 kV, Cell No. 2 was used for measurement of pulses peaking at up to 100 kV. To prevent external flashover, the cell (except for its windows) was encapsulated in silicone rubber compound before working with voltages higher than 60 kV. It should be noted, however, that exposure to such high field strengths is not recommended because of the increased probability of internal corona or flashover. These hazards should be avoided by using cells of greater interelectrode distance at higher voltages.

Because of its large Kerr constant and relatively high dielectric strength, nitrobenzene is used in the Kerr cells. In order to reduce space charge effects and minimize the probability of electrical breakdown in the cell, nitrobenzene of high purity is necessary. Measurements were therefore conducted to determine the resistivity (which increases with purity) of commercially available nitrobenzene. Direct voltage, which rose exponentially to a peak (100 to 3000 volts depending upon the level of current passed by the cell) in a few seconds and then remained constant, was applied to cells filled with various grades of nitrobenzene. The waveform of the applied voltage may be seen from the oscilloscope tracing V in Fig. 2. Measurements performed with nitrobenzene of inadequate purity showed that the current i passed by the cell (see typical result in bottom trace of Fig. 2) is initially quite large ($\sim 20 \mu\text{A}$), that it obeys Ohm's law, and that it decreases very slowly over a period of hours. If voltage is applied for several minutes, removed for several minutes, and then reapplied, the current is found to be substantially the same as before. The resistivity determined from these measurements was of the order of 10^7 ohm-cm. Since resistivities as high as 10^{10} ohm-cm have been reported [9], further purification was undertaken.

After evaluation and experimentation with various methods and combinations of methods of purification [9 through 13], a selective adsorption technique was adopted. In this process, nitrobenzene is

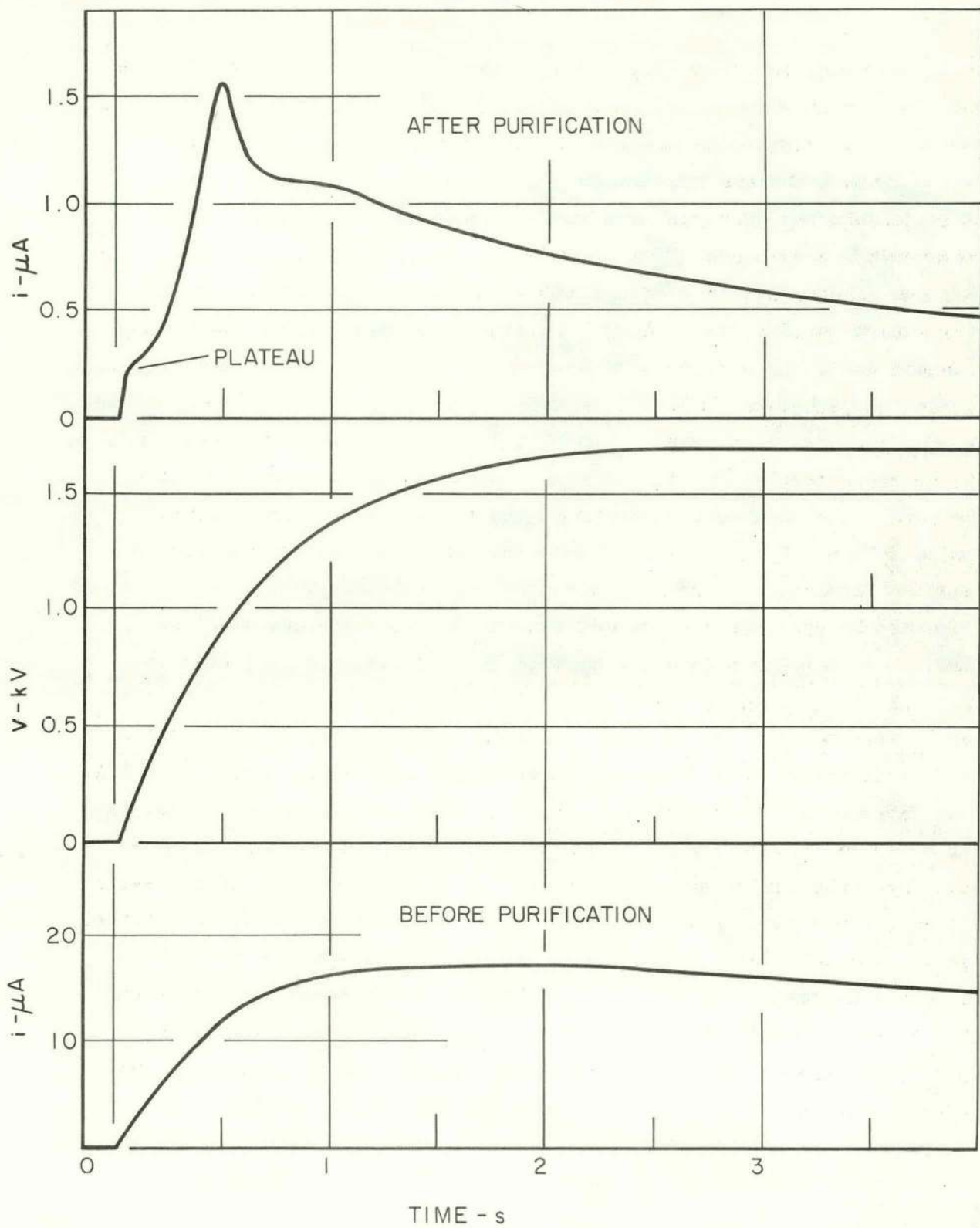


Fig. 2. Time-resolved measurements of voltage (V) and current (i) before and after purification of nitrobenzene.

passed through an adsorption column (length \approx 300 mm, diameter \approx 28 mm) of alumina* as shown schematically in Fig. 3. A sealed vacuum system is used to draw the liquid downward through the column and into the Kerr cell. This technique reduces the time required for filling a cell considerably and prevents recontamination by prolonged exposure to atmospheric conditions. The vapor hazard due to the toxicity of nitrobenzene is also overcome by use of the sealed system and by placing the entire purification and cell-filling apparatus under a laboratory exhaust hood. In addition, all materials used in the apparatus, including glass, polyethylene, Teflon (the stopcocks), nickel (the cell electrodes), Kovar (glass to metal seals), and Viton (O-ring seal), were tested and found to be stable in spite of the strong solvent properties of nitrobenzene. The various components of the system were interconnected by polyethylene tubing. A simple technique was developed to facilitate sealing between the glass and polyethylene members. These seals were effected by pressing the warmed, tapered end of each tubular glass section into polyethylene tubing with I.D. slightly smaller than the O.D. of the glass tube. The polyethylene softens on contact with the warm (near melting point) glass and then contracts around the tapered end as it cools, thus forming a vacuum-tight seal as illustrated in Fig. 4. Sections of the polyethylene tubing were also stretched (by heating) in order to provide the flexibility required for easy manipulation of the Kerr cell during the flushing and filling processes. (If the system is entirely rigid, these processes are complicated by pockets of trapped gas.) The cellulose filter beneath the chromatographic column was inserted to trap alumina particles which pass between the column and the fritted disc.[†] The glass section used for temporary storage of purified nitrobenzene provides a chamber where gases dissolved in the nitrobenzene are boiled off as the liquid comes under stronger vacuum. These sections are shown attached to the chromatographic column in Fig. 5.

*Woelum neutral alumina, activity grade I, purchased from Alupharm Chemicals, New Orleans, Louisiana.

[†]Porosity: coarse.

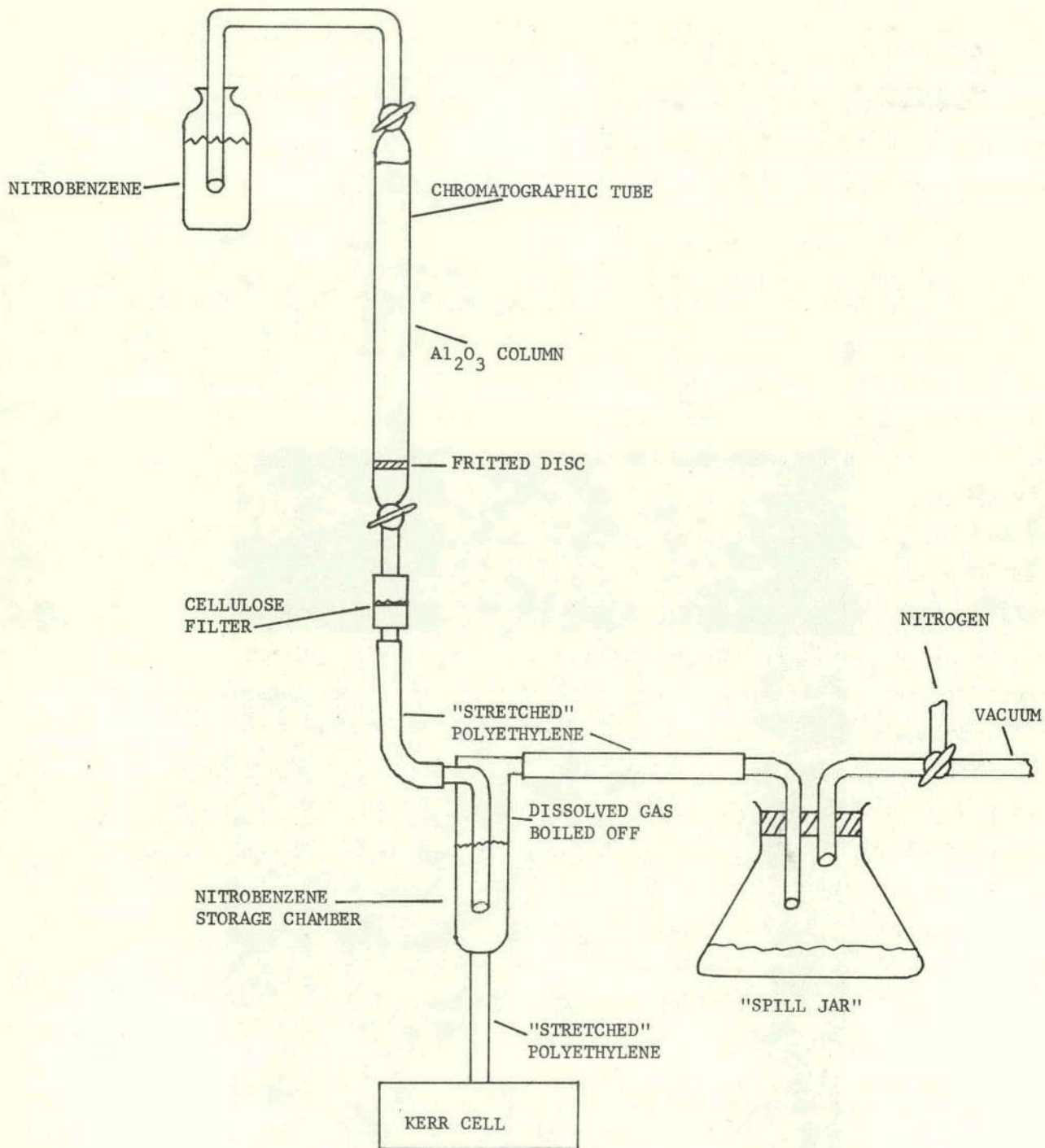


Fig. 3. Apparatus used for purification of nitrobenzene and filling of Kerr cell.

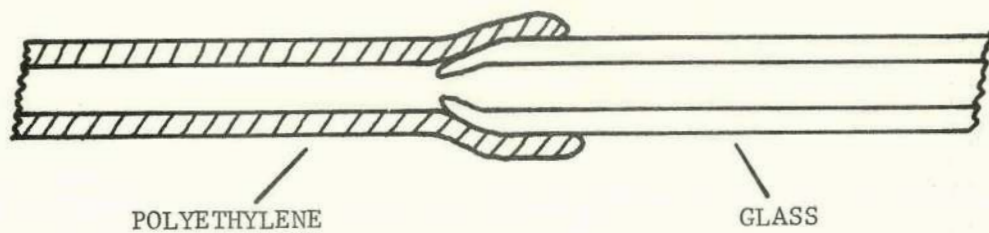


Fig. 4. Glass to polyethylene seal used in purification and cell-filling system.

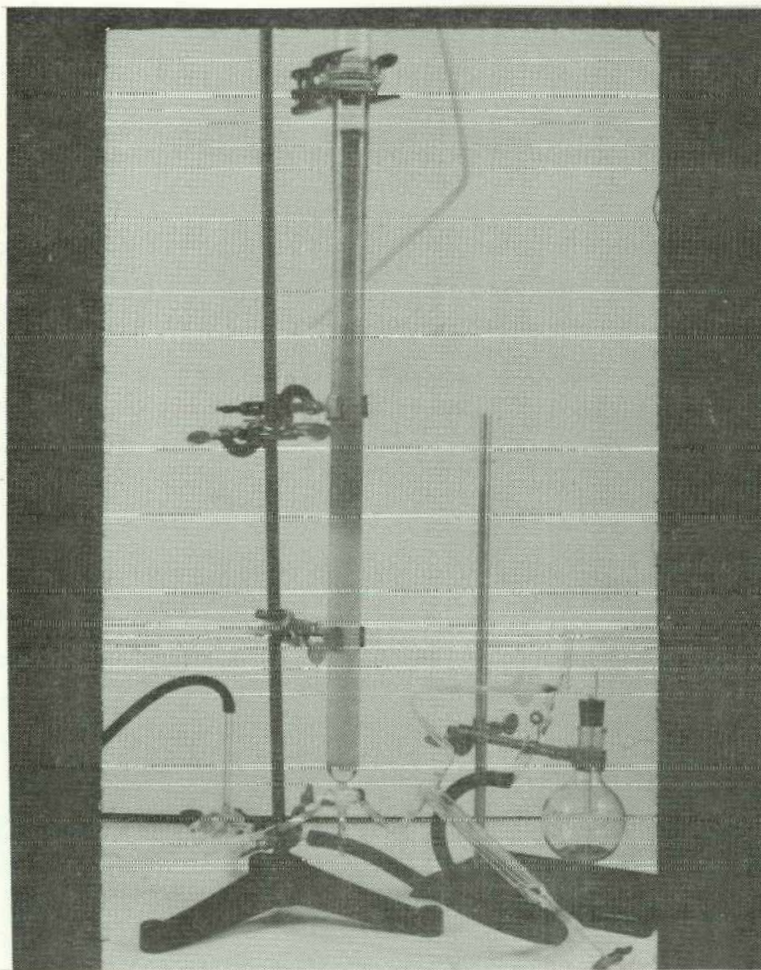


Fig. 5. The chromatographic adsorption column after passage and purification of nitrobenzene.

As the liquid passes through the column, purification is achieved by selective adsorption, with the impurities collecting in distinct, brilliantly colored (red, yellow, brown, etc.) layers of the alumina as shown in Fig. 5. It should be noted that the initial quantities of nitrobenzene passed through a system (including the cell) are contaminated by foreign matter in the system itself, and that they are therefore to be discarded until adequate purity is achieved. In the present work, the cell's resistance, and thus the relative purity of the nitrobenzene, is checked repeatedly by use of the circuit sketched in Fig. 6. In this case, a low voltage square wave of adjustable frequency, rather than a high direct voltage, is applied to the cell, thus circumventing the hazard of working with dangerous voltages while the cell is installed as an integral part of the purification system. Measurements of the cell resistance R are obtained as follows. The cell capacitance and cathode follower input capacitance ($C + C_{CF}$) are determined by applying a high frequency square wave at the input of the circuit and observing the amplitude of the leading edge of the output wave on an oscilloscope. The switch S is closed during this observation. S is then opened and the variable capacitance C' is adjusted until the leading edge of the output waveform is reduced to one half its original amplitude. At this point, $C' = (C + C_{CF})$, and $(C + C_{CF})$ may be read from the scale of the adjustable capacitor C' . The frequency of the applied square wave is then reduced until the decay time τ of each output waveform covers approximately two thirds of the total amplitude as per the sketch in Fig. 6, i.e., until τ is approximately equal to the time constant of the circuit

$$\tau = R[C' + (C + C_{CF})] . \quad (1)$$

Then knowing τ from the frequency f of the input waveform:

$$\tau = \frac{1}{2f} , \quad (2)$$

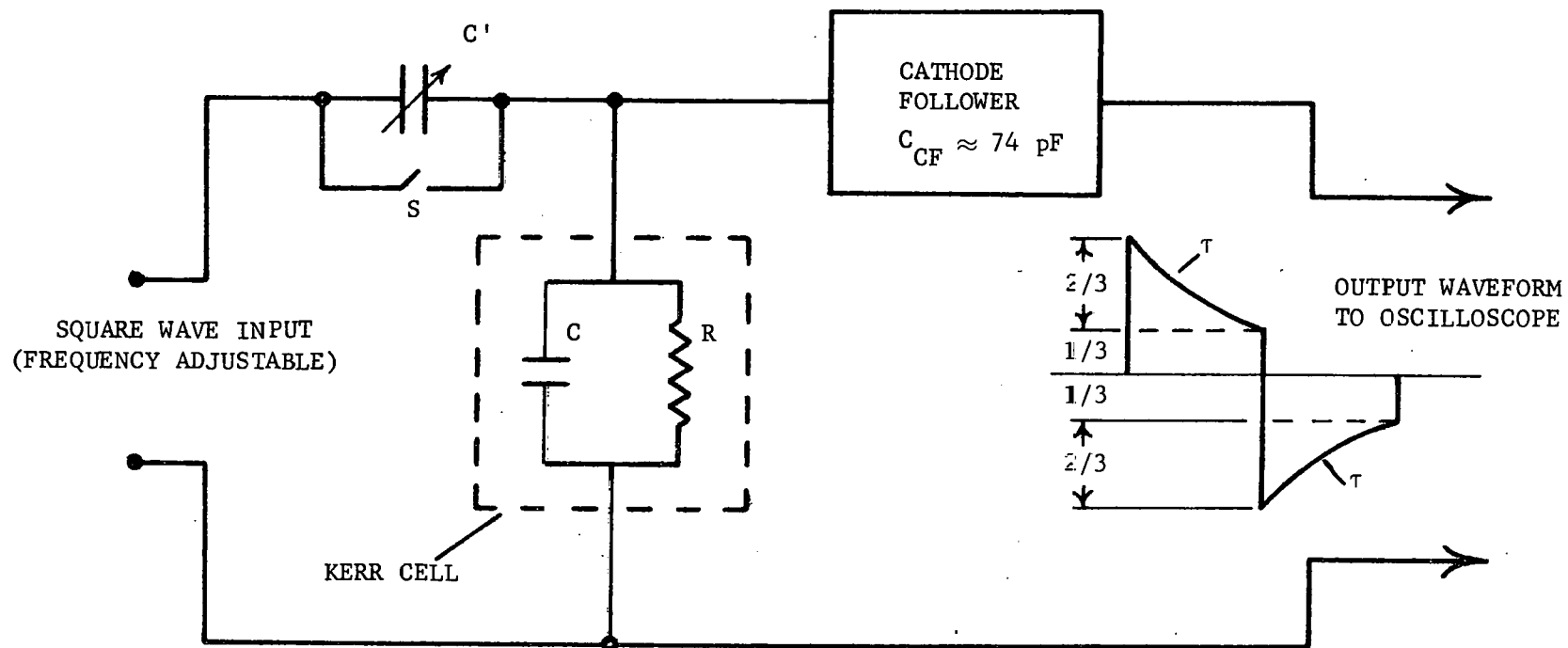


Fig. 6. Circuit used for repeated determinations of Kerr cell resistance during purification process.

the resistance R of the cell is determined from the following equation:

$$R = \frac{1}{2f[C' + (C + C_{CF})]} \quad (3)$$

As the cell's resistance increases (with increasing nitrobenzene purity), the input square wave is adjusted to lower frequencies in order to maintain an output signal with the waveform sketched in Fig. 6. In practice, therefore, the relative purity of the nitrobenzene is detected by monitoring the frequency of the input square wave. With our present cells (which are of approximately the same capacitance ≈ 200 pF) and circuitry, experience indicated that high purity nitrobenzene was obtained when $f < 100$ Hz.

When these tests indicate that the cell is filled with high purity nitrobenzene, the current passed by the cell upon application of a high (up to 15 kV) direct voltage is measured. This measurement serves to detect changes in the purity of the nitrobenzene when the cell is subject to high voltages. The procedure during these tests is essentially the same as described on page 9, except that much higher voltages may now be applied without significantly increasing the current passed by the cell. The top trace in Fig. 2 is typical of a current measurement after adequate purification. In contrast to the behavior indicated by the bottom trace, the current rises rapidly, reaches a plateau which seems to depend in duration upon the spacing between the cell electrodes, increases rapidly to a peak value, drops sharply, and then decreases slowly (in several minutes) to a minimum value ($< 0.5 \mu\text{A}$) where it remains essentially constant. After this point is reached, additional increases in the applied voltage do not cause proportionate increases in the current; the current increases only momentarily and then falls quickly to the former minimum constant value. It was also found that the peak current is strongly dependent upon the time between voltage applications, the peak value being smaller when this time interval was shorter. However, after a few minutes of "conditioning" at several thousand volts, the current falls slowly to the low, nearly constant value observed previously.

In summary, since nitrobenzene of higher purity than is available commercially is necessary, further purification was achieved by passing nitrobenzene (under vacuum) through a chromatographic column of neutral alumina directly into the cell. Initial quantities of the processed nitrobenzene are used to wash the cell and are then discarded until measurements of the current passed by the cell upon application of a high direct voltage indicate that adequate purification has been achieved. The following criteria were found helpful in this procedure: (1) when purity is not adequate, the conduction is ohmic, and the current is relatively large and independent of the time interval between voltage applications; (2) when purity is satisfactory, the conduction is nonohmic, the peak current is smaller and strongly dependent upon the time interval between voltage applications, and the current, after a few minutes of high-voltage "conditioning", remains stable at a relatively low level ($<0.5 \mu\text{A}$) indicative of a resistivity of the order of 10^{10} ohm-cm. After adequate purity is achieved, the cell is filled (under vacuum) with the processed liquid and sealed. Small volumes, charged with dry nitrogen (pressure ≈ 1 atm), are allowed inside the filling ports to permit expansion.

III. ELECTRICAL INSTRUMENTATION AND PROCEDURE

The electrical triggering, delay and measuring instrumentation used for most of the experiments is sketched in Fig. 7. With this arrangement, a high-voltage pulse (peak amplitude from 5 to 100 kV, duration $\approx 15 \mu\text{s}$), produced by a pulse-forming Marx-type generator (impedance 500 ohms), was applied simultaneously to the Kerr cell and to a calibrated pulse divider. The latter, which matched the generator impedance, was made up of five low-time constant, metal ribbon resistors with low voltage coefficients [14].

Time-resolved divider measurements of the pulse were obtained by applying the voltage across the low side of the divider to the +A input of a differential oscilloscope preamplifier. The top waveform v_D in Fig. 8 is a tracing from a typical oscilloscope record. For precision pulse

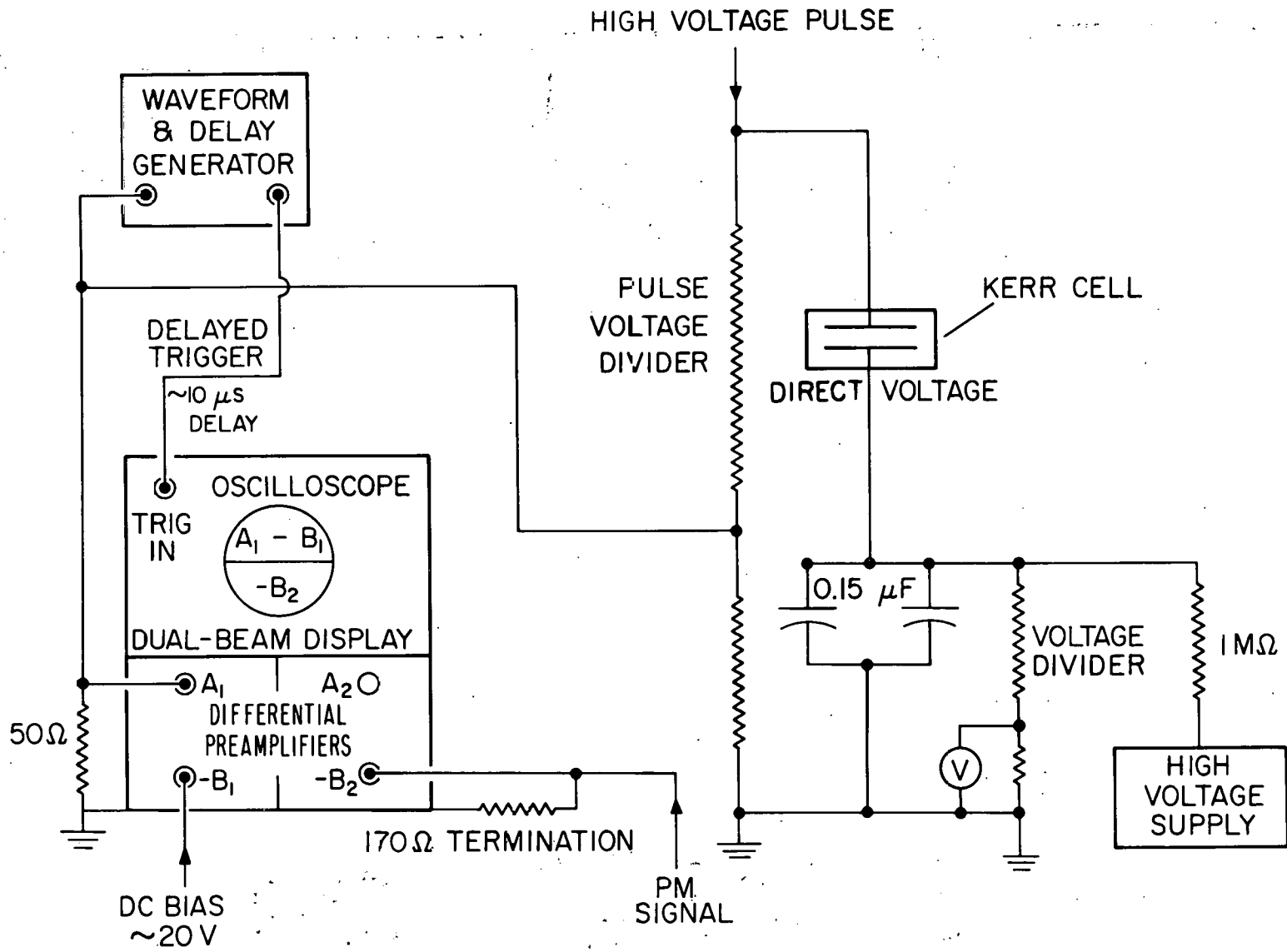


Fig. 7. SCHEMATIC-BLOCK DIAGRAM OF THE ELECTRICAL TRIGGERING, DELAY, AND MEASUREMENTS CIRCUITS.

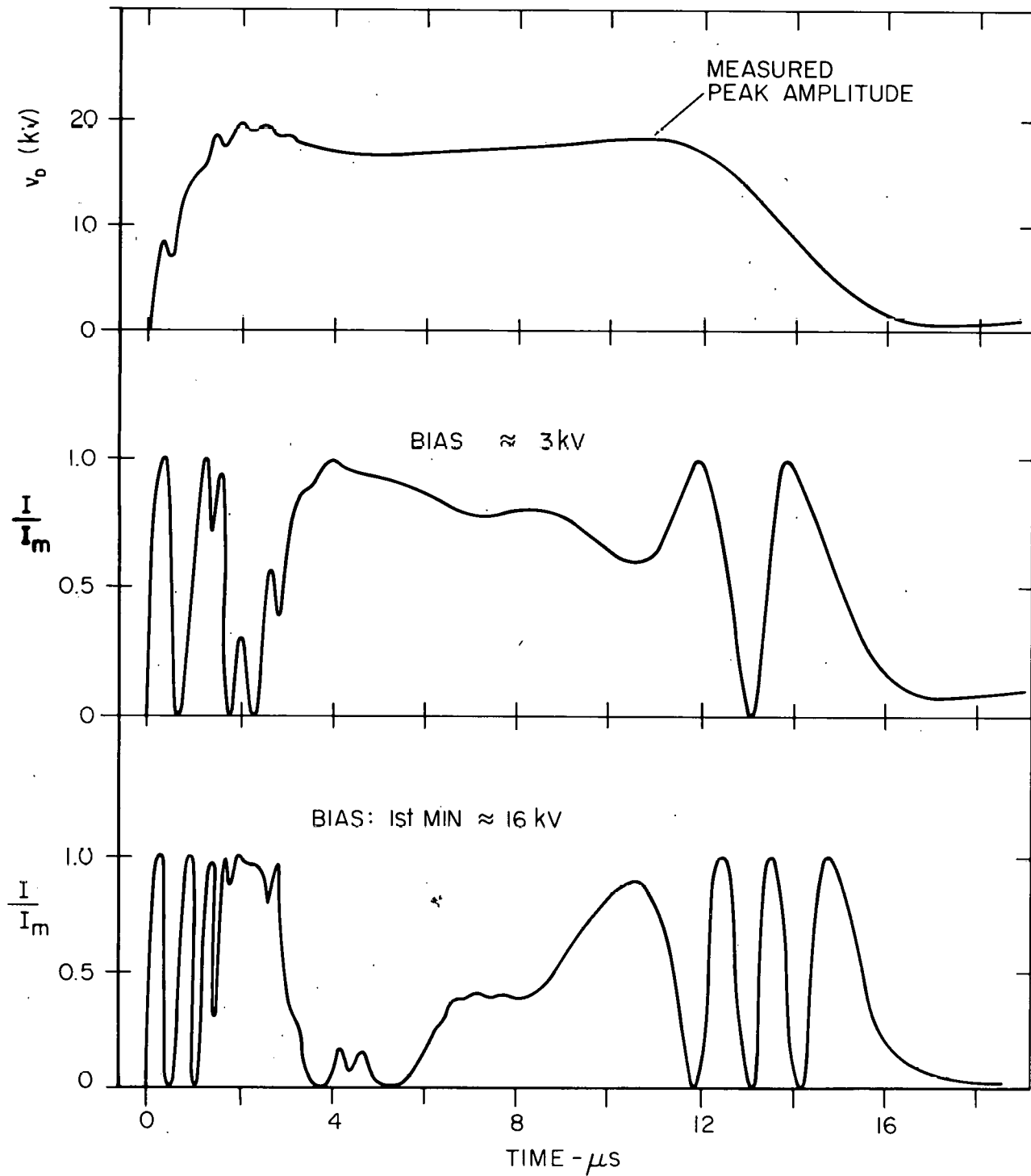


Fig. 8. Voltage divider and Kerr cell measurements of a 20 kV pulse.

divider measurements, a direct voltage approximately equal to (10 to 100 mV less than) the peak amplitude of the "low-side" voltage, was applied to the -B input of the differential preamplifier. The oscilloscope thus recorded (A - B) or v_S , v_S being the difference between the direct voltage and the voltage across the "low side" of the pulse divider. The divider measurement was calculated from the following relation:

$$v_D = DR[v_S + \text{BIAS}] \quad (4)$$

where DR is the pulse divider ratio and BIAS is the direct voltage applied to the -B input as measured with a precision digital voltmeter. The waveform and delay generators provided adjustable triggering of the oscilloscope sweep, thus facilitating expansion of the time scale by adjustment of the horizontal amplifier gain so that the measured peak (just prior to the trailing edge--see Fig. 7) of the pulse could be viewed in detail on the oscilloscope screen. The top trace in Fig. 9 shows a typical record of v_S . Measurements v_D of the peak amplitude made in this way are believed to be accurate to better than 1%.

The optical layout of the Kerr cell-pulse measuring system is shown schematically in Fig. 10. The cell is installed between "crossed" polarizers so that no light is transmitted until voltage is applied. A laser (helium-neon, wavelength: 632.8 nm) beam is directed through the cell, between and along the length of the plate-electrodes, to a well-shielded photomultiplier tube.* The components are aligned with considerable care and black felt squares, with holes (diam. \approx 1 cm) for passage of the beam, are mounted over the inner faces of the polarizer holders in order to minimize and attenuate reflections. Appropriate Neutral Density Filters are often inserted in the optical path as indicated to prevent overloading of the photomultiplier circuit. The negative lens serves to spread out the laser light over the photosensitive surface. Careful alignment of the light-tight tube, which keeps out extraneous room light, is necessary to insure

*Type 5819 with conventional supply and divider circuits.

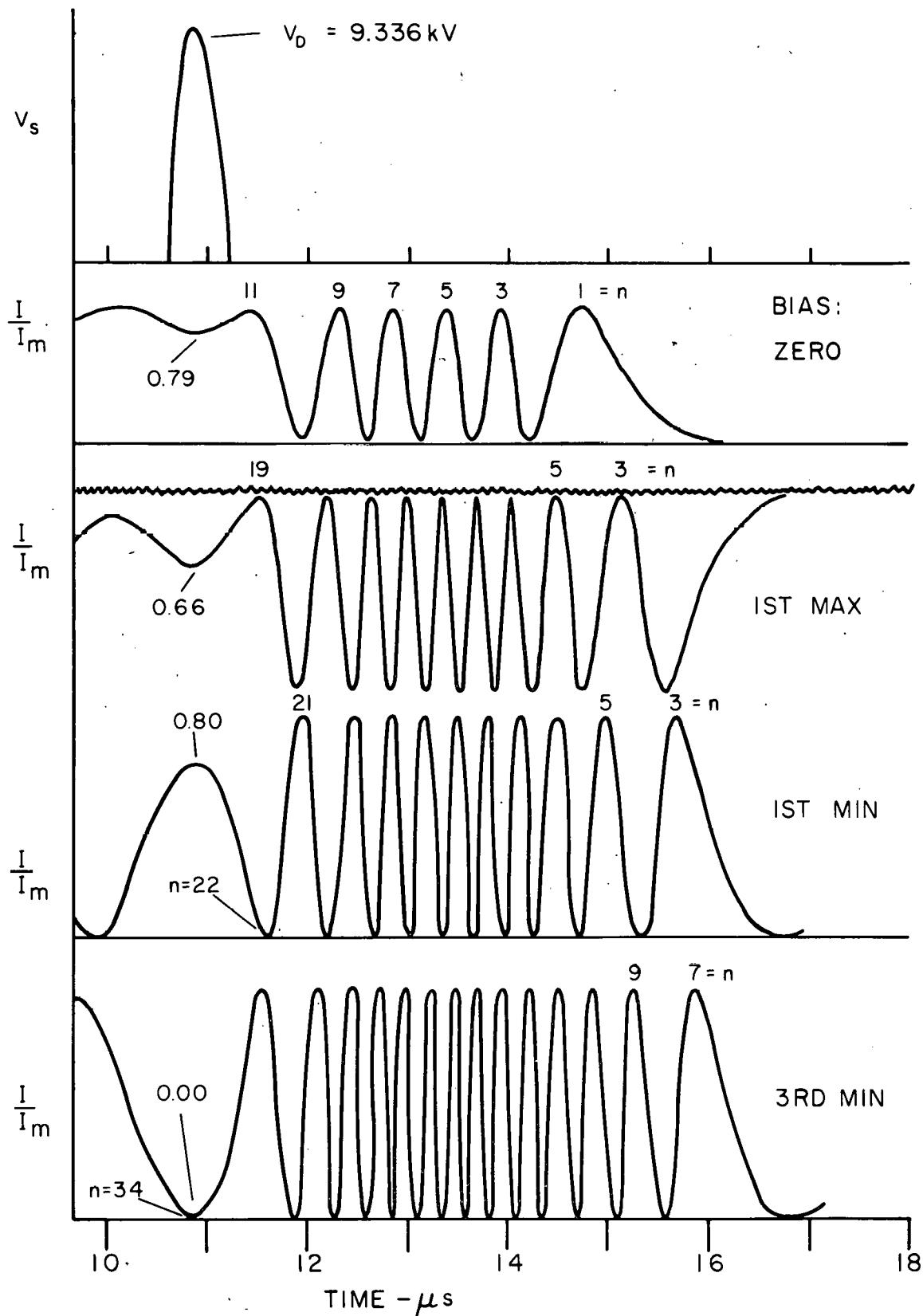


Fig. 9. Calibrated voltage divider (top) and Kerr cell measurements of peak amplitude of a high voltage pulse.

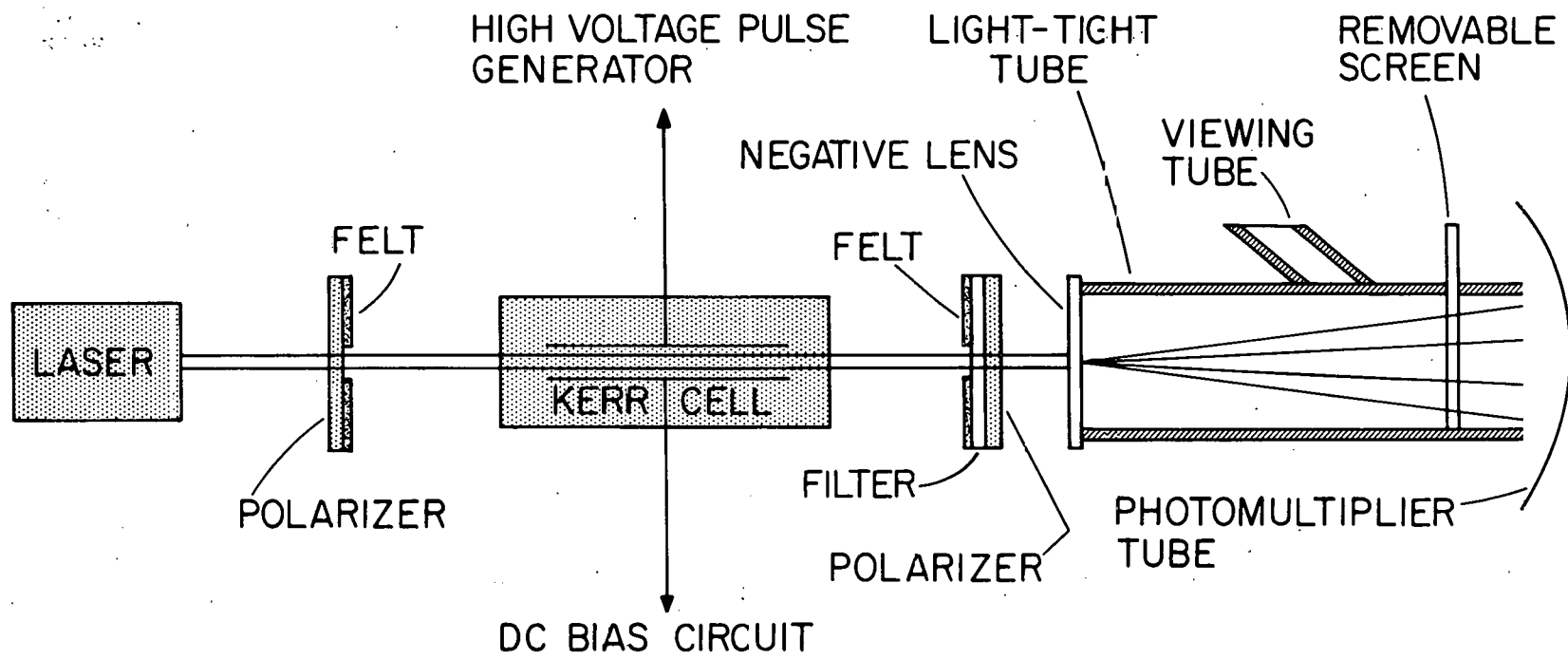


Fig. 10. LAYOUT OF THE OPTICAL SYSTEM

passage of most of the diverging laser beam (rather than its reflections from the inner wall of the tube) to the photomultiplier. The viewing tube close to the photomultiplier end of the light-tight tube permits observation of the beam's reflection on a removable screen during calibration experiments. This screen is removed and the viewing port is capped during pulse measurement experiments. In most experiments, a direct voltage, which biases the system to its first transmission minimum, was applied to the cell. In the present setup, since the pulses to be measured are of positive polarity with respect to ground, a negative voltage is applied to the lower electrode (see Figs. 1 and 7) of the Kerr cell, so that the bias is added to the voltage difference imposed across the cell by the positive pulse. This voltage serves several purposes: (1) it reduces the danger of internal arcing by "conditioning" the cell for application of high voltage; (2) it increases the sensitivity of the Kerr system (more oscillations of the transmitted intensity are produced by a given pulse voltage); and (3) it enables calibration of the system without reference to pulse divider measurements; as described in Sections VI-B and VI-C.

When voltage is applied across the cell electrodes, the state of polarization of the beam is altered (the Kerr effect), thus causing variations in the intensity of the transmitted light. The transmitted intensity I at any instant is dependent upon the strength E of the electric field imposed by the applied voltage as follows [5,8]:

$$(I/I_m) = \sin^2 \frac{\pi}{2} (E/E_m)^2 \quad (5)$$

where I_m is the maximum intensity transmitted by the system and E_m is the field strength required to produce the first transmission maximum. The relative intensity (I/I_m) of the transmitted beam as a function of relative field strength (E/E_m) , as computed by use of Eq. 5, is shown graphically in Fig. 11. Maximum transmission will occur when $(E/E_m) = 1, \sqrt{3}, \sqrt{5}, \text{etc.}$, and minimum transmission will occur when $(E/E_m) = 0, \sqrt{2}, \sqrt{4}, \text{etc.}$

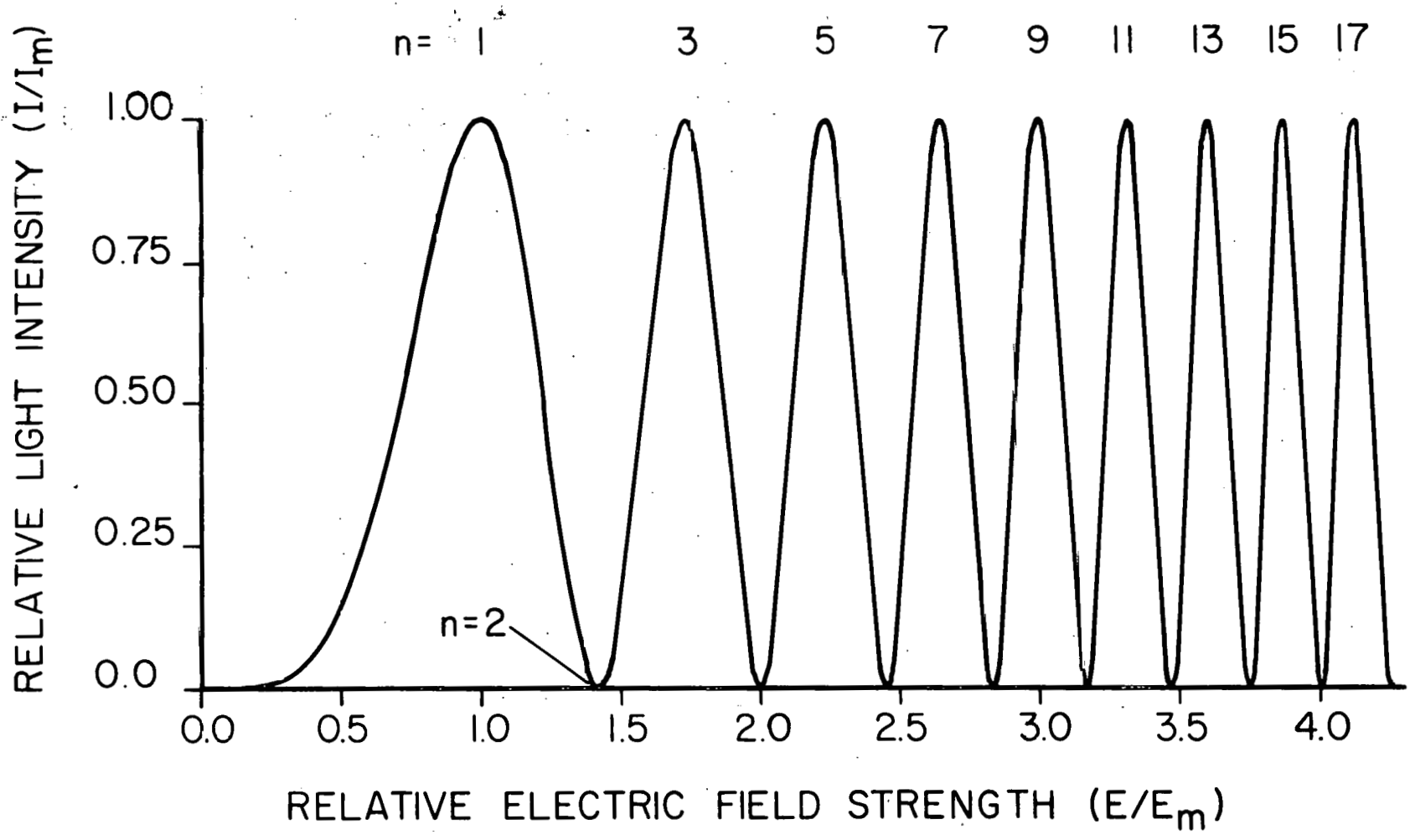


Fig. 11. Relative transmitted light intensity vs. relative field strength with numerical values assigned to successive transmission maxima and minima.

Thus, the relative strength (E/E_m) of the field imposed by an applied voltage may be determined from a time-resolved oscilloscope record of the photomultiplier's response to the modulated beam intensity as follows: If the relative intensity is increasing at the instant of measurement,

$$(E/E_m) = [n + \frac{2}{\pi} \arcsin (I/I_m)^{\frac{1}{2}}]^{\frac{1}{2}}, \quad (6)$$

where n is the number of maxima and minima traced by the waveform prior to the instant of measurement, and (I/I_m) is the relative intensity of the beam at the instant of measurement. If (I/I_m) is decreasing at the instant of measurement,

$$(E/E_m) = [(n + 1) - \frac{2}{\pi} \arcsin (I/I_m)^{\frac{1}{2}}]^{\frac{1}{2}}. \quad (7)$$

The applied voltage V is determined from this ratio (E/E_m) by use of the following equation:

$$V = (E/E_m)(E_m d), \quad (8)$$

where the product $(E_m d)$ of the field strength E_m required to produce maximum transmission and the interelectrode distance d is the cell constant. Determination of this quantity $(E_m d)$ constitutes calibration of the system. In the present work, calibrations of the cell with relatively small interelectrode spacing (~ 0.25 cm) were achieved by the methods described in Section IV. In this case, the field imposed by an applied voltage was assumed to be uniform since little evidence of field distortion was observed. However, the two cells with greater electrode spacing (0.75 cm) exhibited significant field distortion effects when direct bias voltage was applied to the cell. In these cases, effective calibrations were achieved by the techniques described in Section VI.

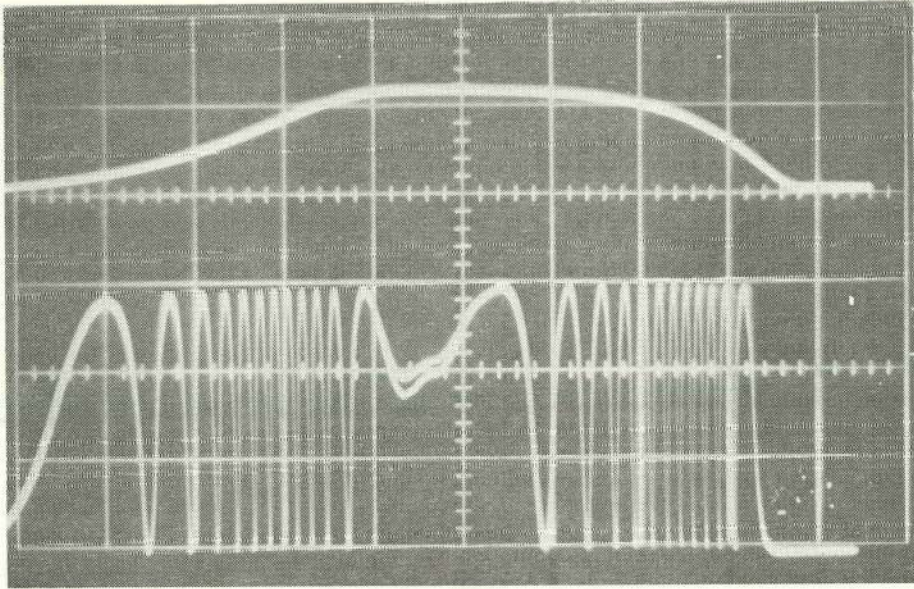
Tracings from typical oscilloscope records are shown in Fig. 9. The top trace v_s (see Eq. 4) gives the divider measurement v_D of the peak amplitude of the pulse. The other traces show (I/I_m) as a function of time over the latter portion of the pulse, including the peak amplitude

point and the trailing edge. Numerical values (n) are assigned to successive maxima and minima as indicated above. These are counted from right to left for convenience, since, as may be seen from Fig. 8, the pulse amplitude at the selected point of measurement occurred just prior to the trailing edge. It should be noted that the value assigned to the first intensity peak (on the right of the record) is affected by the bias voltage. When the cell is biased to the first, second, or third transmission minimum, this peak is indicative of $n = 3, 5, \text{ or } 7$, respectively. The traces were obtained with no bias voltage applied (second trace), and with applied direct bias voltages which produced the first transmission maximum, the first minimum, and the third minimum (third, fourth, and fifth traces, respectively). The higher values of n prior to the peak of the pulse ($n = 19, 22, 33$) demonstrate the increased sensitivity of the system at higher bias levels. Superimposed pulse divider measurements are compared with superimposed Kerr system results (obtained with another Kerr system) in Fig. 12. The peak amplitude of the superimposed pulses differed by 0.1% (peak amplitudes in the top records 142,295 volts and 142,443 volts) and by 1% (peak amplitudes in the bottom records 142,295 volts and 143,782 volts). The superior measurement resolution afforded by the Kerr cell system, as compared to that obtained with conventional pulse divider techniques, is evident; indications of the peak amplitude differences are not detectable in the divider records, whereas sizable differences are noted in the Kerr cell records.

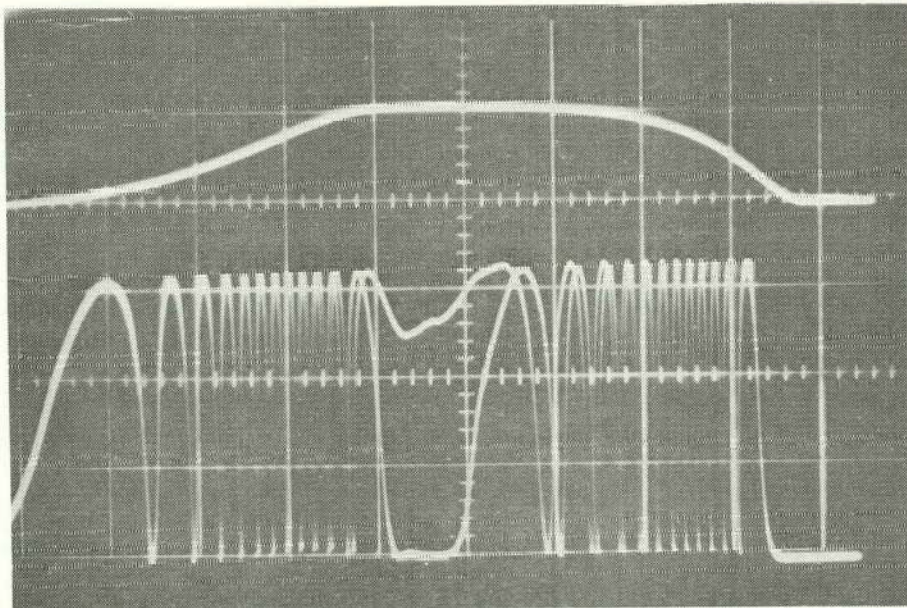
IV. CALIBRATION WITH A UNIFORM FIELD

As stated above, assumption of a uniform interelectrode field distribution did not introduce serious error when a Kerr cell having relatively small (~ 0.25 cm) electrode spacing, filled with highly purified nitrobenzene, was used. In this case, several straightforward methods of calibration were found to be valid, including the following:

DOUBLE TRACES



DIFFERENCE IN PEAK AMPLITUDE: 0.1%



DIFFERENCE IN PEAK AMPLITUDE: 1.0%

Fig. 12. Superimposed pulse divider (top traces in each record) and Kerr system (bottom traces) measurements.

A. Pulse Divider Techniques

If no bias voltage is applied, the cell constant $(E_m d)$ may be obtained quite simply from simultaneous calibrated divider and Kerr system measurements by use of the following equation:

$$(E_m d) = \frac{v_D}{(E/E_m)}, \quad (9)$$

where v_D is the divider measurement derived from Eq. 4, and (E/E_m) is derived from the photomultiplier record of n and (I/I_m) using Eq. 6 or 7. Accuracy in the calibration is limited only by the accuracy of the calibrated divider ratio and by error in reading of (I/I_m) from the oscilloscope record. In the present work, it is estimated that these errors did not exceed 1%.

If a bias voltage is applied to the cell, $(E_m d)$ may be determined from the following equation:

$$(E_m d) = \frac{v_D + V_{BIAS}}{(E/E_m)}, \quad (10)$$

In the present work, the direct voltage V_{BIAS} , which was measured to within 0.01% by use of a resistive divider, was adjusted until the first, second, or third transmission minimum was observed visually. The first peak of the pulse-induced photomultiplier record was thus indicative of $n = 3, 5, \text{ or } 7$, respectively; and (E/E_m) was the total relative field strength imposed by the pulse and bias voltages. Values of $(E_m d)$ determined in this way are subject to the same errors as in the above case, the principal limitation in both cases being their dependence upon the calibrated pulse divider measurements.

B. Two-Pulse Technique

Reference to pulse divider measurements may be avoided by applying two identical pulses ($v_1 = v_2$) to the cell while it is biased first at one and then at another voltage. The total voltages across the cell are thus:

$$V_1 = v_1 + V_{\text{BIAS1}} \quad \text{and} \quad V_2 = v_2 + V_{\text{BIAS2}}, \quad (11)$$

and the cell constant may be written

$$(E_m d) = \frac{V_{\text{BIAS1}} - V_{\text{BIAS2}}}{(E_1/E_m) - (E_2/E_m)}, \quad (12)$$

with all parameters measured as in Method [IV-A] and with the added advantage that pulse divider measurements are not required. Significant errors may be averted by making every feasible effort to satisfy the following criteria: (1) the pulses applied must be identical, and (2) factors contributing to error in the difference $[(E_1/E_m) - (E_2/E_m)]$ must be minimized. To achieve the latter, the oscilloscope's vertical amplifier may be adjusted to yield maximum deflection for I_m on the oscilloscope screen; V_{BIAS1} may be made as high as is feasible with a given cell; and V_{BIAS2} may be made as low as feasible (zero if no bias is desired for "conditioning" purposes).

Evaluation of this technique suggests several sources of error:

(1) If v_1 and v_2 are not identical, one should expect an error as follows:

$$\Delta_{v_1 \neq v_2} = \frac{-100 \delta v_1}{V_{\text{BIAS1}} - V_{\text{BIAS2}} - \delta v_1} \quad (13)$$

where δ is the proportional difference between v_1 and v_2 and $\Delta_{v_1 \neq v_2}$ is the percentage error in the determined value of $(E_m d)$. (2) It is evident from inspection that the accuracy of $(E_m d)$ will be increased when the difference between the bias voltages is maximized. (3) When reasonable care is exercised (I_1/I_m) and (I_2/I_m), from which (E_1/E_m) and (E_2/E_m) are determined, can be measured from an oscillogram with relative ease to $\pm 0.05 I_m$. For measurements with $n > 2$, such an error would in most cases introduce errors considerably smaller than 0.03 or 1% in (E/E_m) , with the errors diminishing as n increases. However, for measurements with I/I_m near a maximum or minimum transmission point, i.e., when

I/I_m is between 0.9 and 1.0 or when $I/I_m = 0$ to 0.1, respectively, percentage errors as large as 4.7% (when $n = 2$) may be introduced in (E/E_m) , with the errors diminishing as n increases. The percentage error $\Delta(E_{1,2}/E_m)$ in $(E_m d)$ due to errors in measurement and/or reading of (I_1/I_m) and (I_2/I_m) may be estimated from the following equation:

$$\Delta(E_{1,2}/E_m) = \frac{100[(E_1/E_m)\delta_1 - (E_2/E_m)\delta_2]}{(E_1/E_m)(1 + \delta_1) - (E_2/E_m)(1 + \delta_2)} \quad (14)$$

where δ_1 and δ_2 are the proportional errors in (E_1/E_m) and (E_2/E_m) . Realistic errors of +0.01 and -0.01 in the latter could therefore cause errors as large as 4.1% in $(E_m d)$.

In view of these points, it is not difficult to accept the deviations noted in Table 1 as typical of calibration results obtained by this method. Rather it is encouraging to note that the actual deviations of $(E_m d)_{IV-B}$ from $(E_m d)_{IV-A}$ were considerably smaller than one might expect. The values of $(E_m d)$ obtained by this method [IV-B] for the 0.25 cm cell, which exhibited little evidence of nonuniformity in its field distribution, differed from pulse divider calibrations [IV-A] by about 2% (see Table 1).

C. Detection and Measurement of Bias at Minimum

Finally, if the field distribution is uniform, independent calibration may be achieved by adjusting the bias voltage until the first, second, or third transmission minimum ($n = 2, 4, \text{ or } 6$) is observed or detected photoelectrically. The cell constant is then calculated from

$$(E_m d) = \frac{V_{\min}}{(E_{\min}/E_m)} \quad (15)$$

where V_{\min} is the bias voltage at which the minimum is observed; and from Eq. 5, $(E_{\min}/E_m) = \sqrt{2}, \sqrt{4}, \text{ or } \sqrt{6}$. Minimum, rather than maximum, transmission points were selected for detection, because perception of the maximum intensity of a high-intensity source is more difficult. Minimum transmission points, on the other hand, were detected quite reproducibly. Best results were obtained with photoelectric detection.

Table 1. Calibrations of a Kerr Cell with Near-Uniform Electric Field Distribution

Kerr System Data					Pulse-Divider Method [IV-A]		Two-Pulse [‡] Method [IV-B]		Method [IV-C]	
Bias Point	V _{BIAS} [volts]	n	(I/I _n)	(E/E _m)	v _D [volts]	(E _m d) [volts]	(E _m d) [volts]	Δ* [%]	(E _m d) [volts]	Δ [†] [%]
Zero	0	11	0.79	3.362	9335	2777	2769	-0.3		
1st Max	2906	19	0.66	4.404	9334	2780	2752	-1.3	2906	+6.0
1st Min	3915	22	0.88	4.772	9329	2776	2762	-0.7	2768	-0.3
2nd Min	5536	28	0.79	5.357	9325	2773	2742	-1.9	2768	-0.3
3rd Min	6809	33	0.04	5.820	9336	2774	Reference		2779	+0.3
2nd Min	5535	28	0.80	5.358	9326	2773	2750	-1.4	2768	-0.4
1st Min	3914	22	0.79	4.764	9343	2782	2742	-2.1	2768	-0.7

*Deviation of cell constant (E_m d) as determined by Method [IV-B] from that determined by Method [IV-A].

†Deviation of (E_m d) as determined by Method [IV-C] from that determined by Method [IV-A].

‡These calibrations are referred to the experiment with the cell biased at the third transmission minimum, i.e., (E₁/E_m) and V_{BIAS1} in Eq. 12 were taken as 5.82 and 6809 volts, respectively.

For maximum sensitivity and minimum error due to drifting of the oscilloscope beam, the cable termination used during pulse measurement experiments was removed during this procedure. This precaution reduced the spread in our detections of the minimum transmission voltage from 1% to about 0.1%. Values of $(E_m d)$ for the cell with $d \approx 0.25$ cm, as determined by this method, deviated from pulse divider calibrations by less than 1%. This method is preferred over methods IV-A and IV-B because it does not require reference to pulse divider measurements. Typical data and results obtained by the methods described in this Section [IV] are presented and compared in Table 1.

V. THE NONUNIFORM ELECTRIC FIELD

Unfortunately, calibrations of the cells with greater interelectrode spacing (~ 0.75 cm) showed significant errors when the foregoing methods were employed. Investigations showed that application of a direct bias voltage produces distortion in the electric field distribution probably because it causes ionic impurities in nitrobenzene to collect near the electrodes. Experiments were therefore performed to investigate the extent of field distortion.

In the first of these experiments, a pinhole aperture, collimating lens and beam expanding telescope,* which expanded the 2 mm diameter beam to a collimated 50 mm beam, were attached to the laser source,† thus causing the beam to cover the entire interelectrode area. The pinhole aperture provided a smooth Gaussian intensity profile across the collimated beam. The image of the electrodes silhouetted by the transmitted beam was observed on and photographed from a ground-glass screen placed between

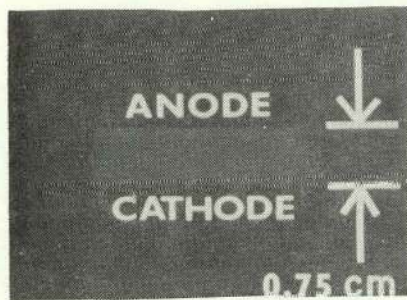
*Spectra-Physics Models 331 and 332.

†Spectra-Physics Model 131.

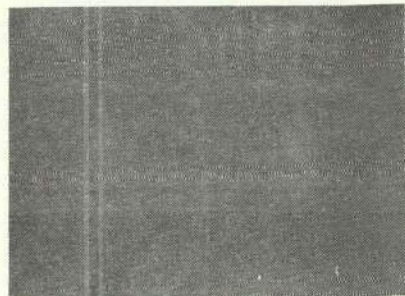
the negative lens and the photomultiplier tube. Typical photographs with various direct voltages applied to Cell No. 1 are shown in Fig. 13. The first photograph (11,075 volts) shows the radiant flux transmitted over the interelectrode area with the bias voltage required for the first transmission maximum (approximately) applied. Upon application of voltages nearer that required for the first transmission minimum, dark regions of low and near-zero transmission were evident in contrast to other regions of relatively high transmission, thus indicating definite regions of different electric field intensity. The region of near-zero transmission, where the field intensity was approximately equal to that (E_{\min}) required for the first minimum of light transmission, first appeared as a narrow dark band parallel to the surface of the cathode at about 12,970 volts. As the applied voltage was increased, the band grew in area, bowed out in the center, and moved toward the anode as shown in the photographs. At any given voltage, the pattern was stable, showing no shifting of the darker regions even over periods of many minutes. Minimum transmission occurred between 15,903 and 16,203 volts (closer to 15,903 volts).

Figure 14 is a "map" (composite taken from these and other similar photographs) of the profile of the electric field distribution over the entire area between the plates. The relative local field intensities (E/E_{\min}) were derived from the proportional changes in voltage required for given shifts in the transmission pattern. The results demonstrate significant nonuniformity in the field strength.

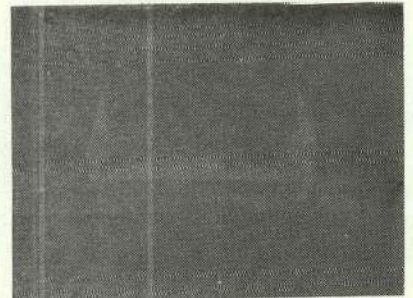
In a second series of experiments investigating the field distribution in Cell No. 1, direct voltage was applied to the cell and the laser source (which was mounted on an adjustable laboratory jack) was moved across the distance between the electrodes. The intensity of the transmitted beam as a function of distance was recorded by applying the photomultiplier's response to the vertical amplifier of an oscilloscope. At the same time, the voltage across the tapped portion of a ten-turn potentiometer, with the tap mechanically linked to the position of the laser beam (i.e., to the supporting jack), was applied to the horizontal amplifier. The gain



11,075 VOLTS



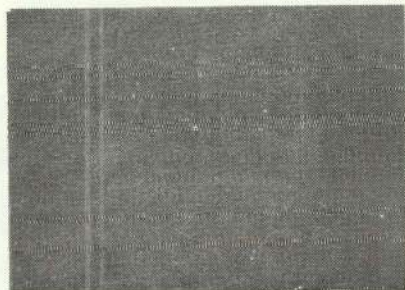
15,570



16,803



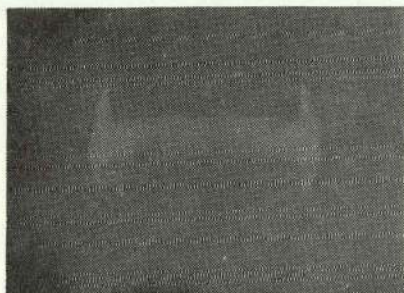
14,402



15,903



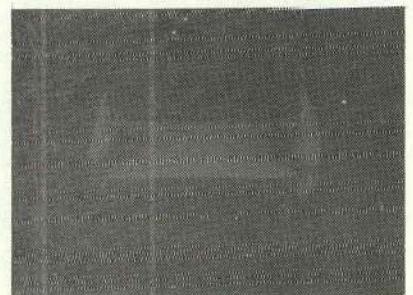
17,103



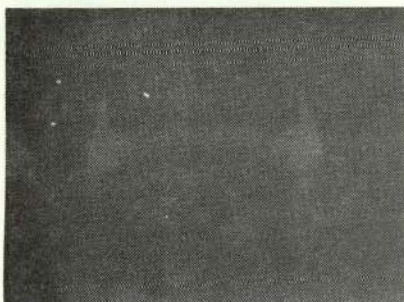
15,003



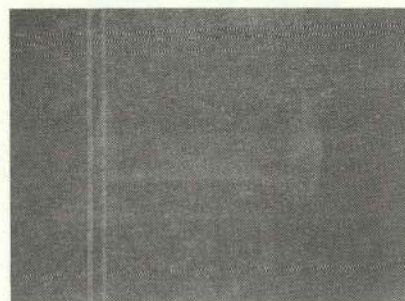
16,203



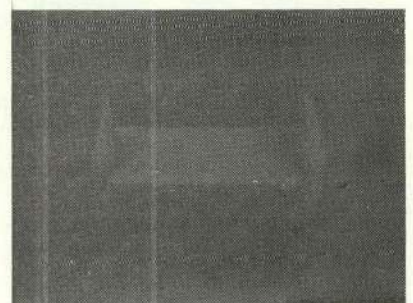
17,403



15,213



16,503



17,853

Fig. 13. Laser photographs showing profile of electric field in Kerr cell.

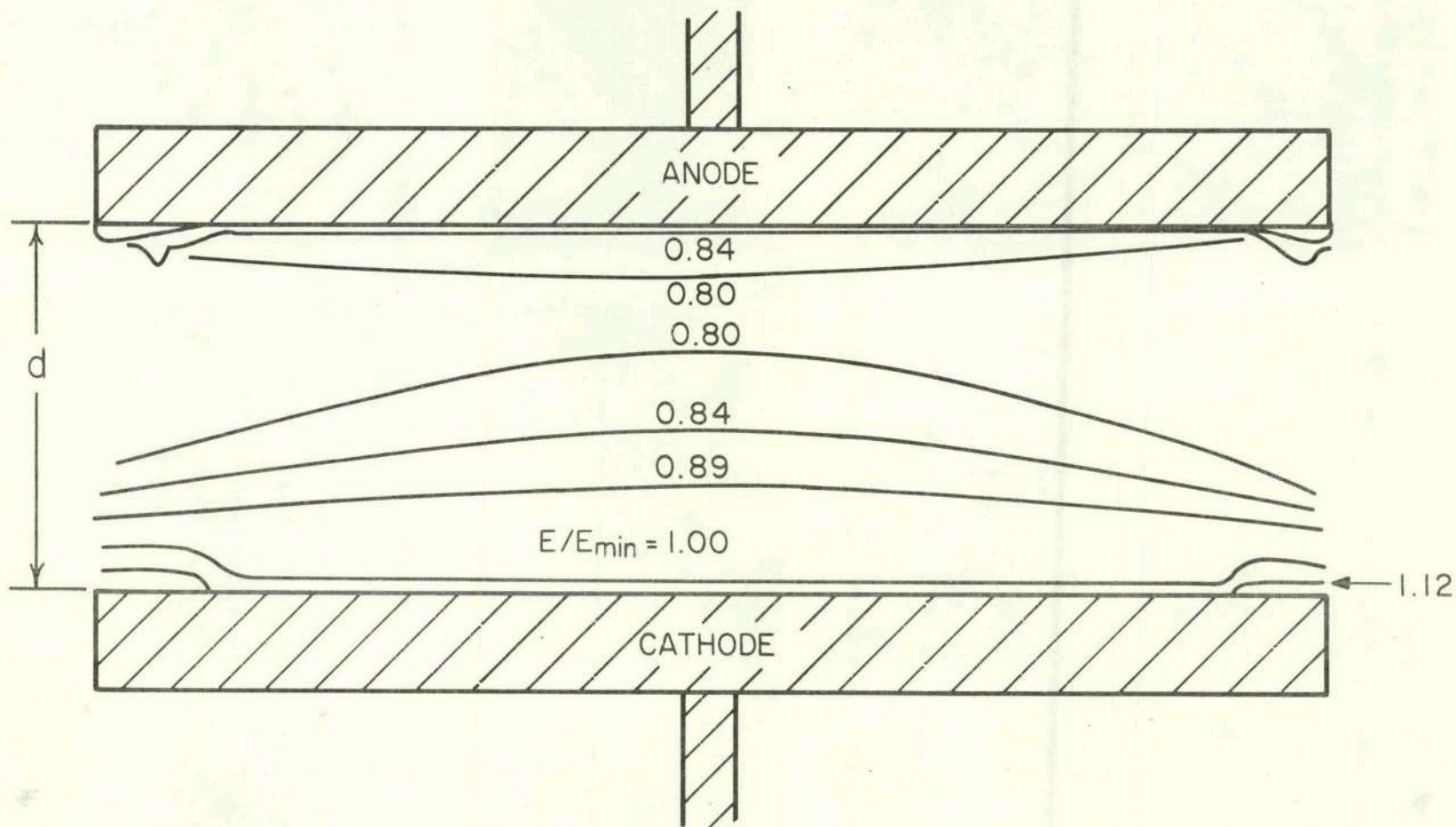


Fig. 14. Profile of the electric field distribution over the interelectrode area of Cell No. 1 ($d \approx 0.75$ cm).

was adjusted so that the travel required to cover the distance between the plates gave full- (horizontal) scale deflection on the oscilloscope. The position of the oscilloscope beam thus gave direct indication of the relative intensity I/I_m of the transmitted beam (on the vertical scale) and the location of the laser beam's path through the Kerr cell (on the horizontal scale). Figure 15 is a composite tracing of oscilloscope records obtained with various voltages (Curves 1 through 7) applied to the cell. Since considerable care is required for interpretation of these measurements, the measured values of I/I_m and n are noted at several positions on Curves 1 and 6 for the convenience of the reader. Curve 7, which gives the level of maximum transmission, was obtained with the polarizer and analyzer "uncrossed" and with no voltage applied to the cell.

The relative field strengths (E/E_m) at various distances from the anode in the cell were derived directly from these measurements of I/I_m and n . Values of (E/E_m) obtained in this way from Curves 1, 2, 5, and 6 are plotted in Fig. 16. (Curves 3 and 4 were omitted for clarity.) The field distribution indicated shows that the field strength was highest near the cathode, lowest at position D, and then higher again near the anode. This distribution is in agreement with that indicated by the experiments of Figs. 14 and 17. It is also important to see that the field distribution did not vary significantly when the applied voltage was changed by as much as 35%.

In a third series of experiments with Cell No. 1, the direct voltage V_{min} which produced the first transmission minimum was measured with the laser beam passed along various paths between the plates. A micrometer coupled with a spring-loaded base, as shown in Fig. 1, was used for adjustment and measurement of the position of each path. Results showing V_{min} as a function of distance was plotted in Fig. 17. Significant distortion of the electric field distribution is evident. Extrapolation of the curve to the electrodes suggested that even greater distortion existed near the electrodes. The following techniques were therefore devised for calibration in the presence of field distortion effects.

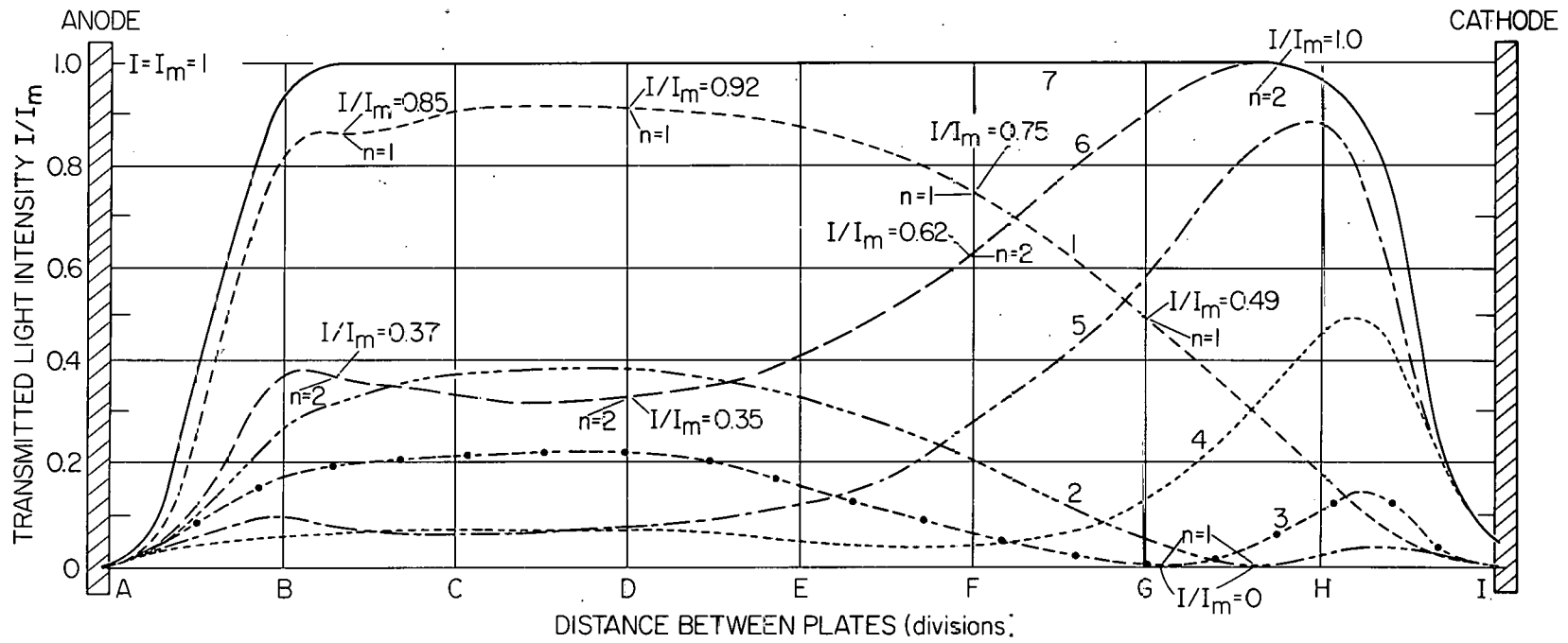


Fig. 15. Relative intensity of transmitted beam as a function of distance between the electrodes of Cell No. 1 as recorded by photomultiplier tube, at various applied voltages: $V_1 = 13,097$, $V_2 = 14,640$, $V_3 = 15,160$, $V_4 = 16,045$, $V_5 = 17,082$, and $V_6 = 18,086$ volts.

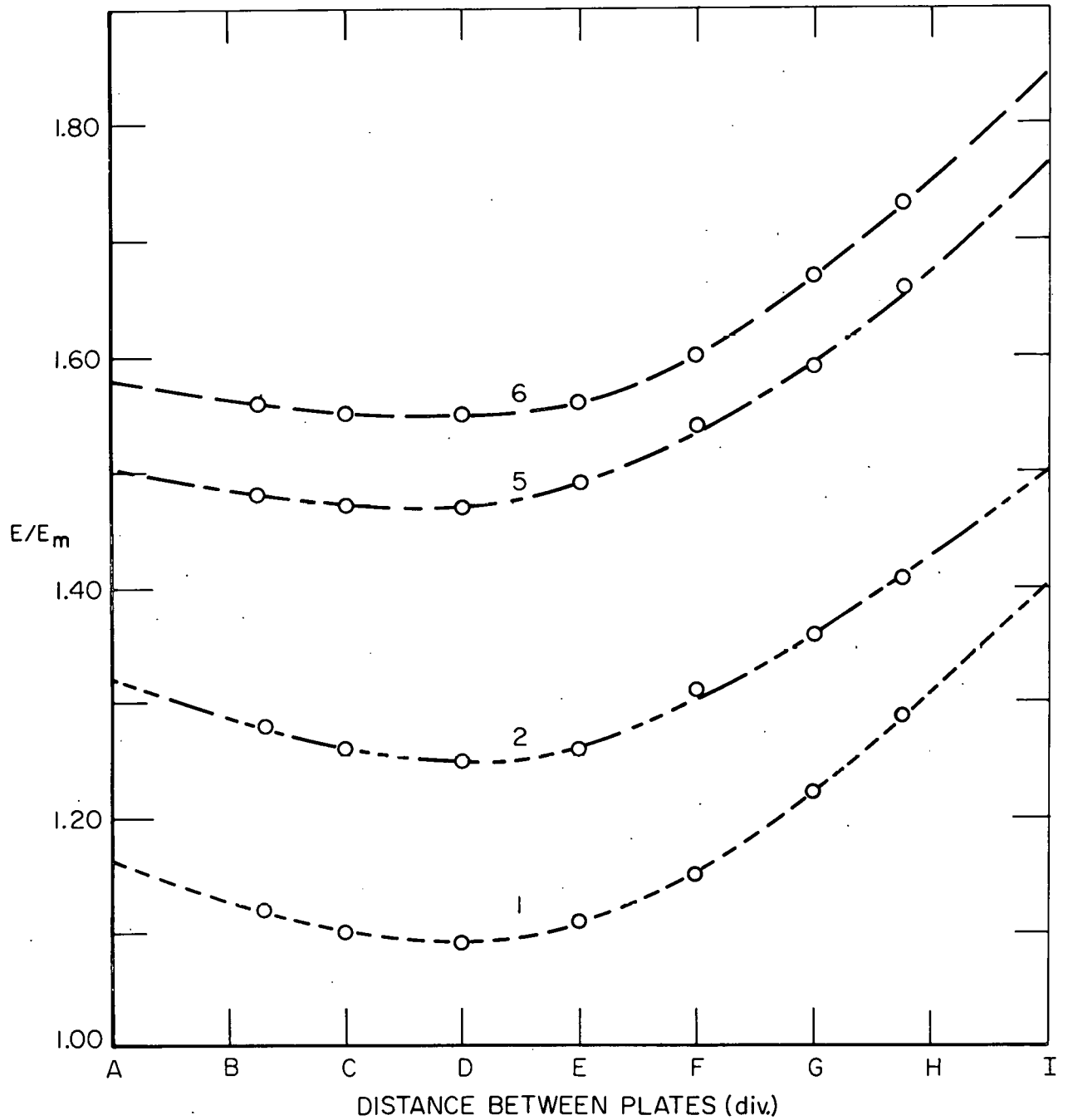


Fig. 16. Relative field strength in Cell No. 1 as a function of interelectrode distance, as derived from the photomultiplier records of I/I_m and n in Fig. 15.

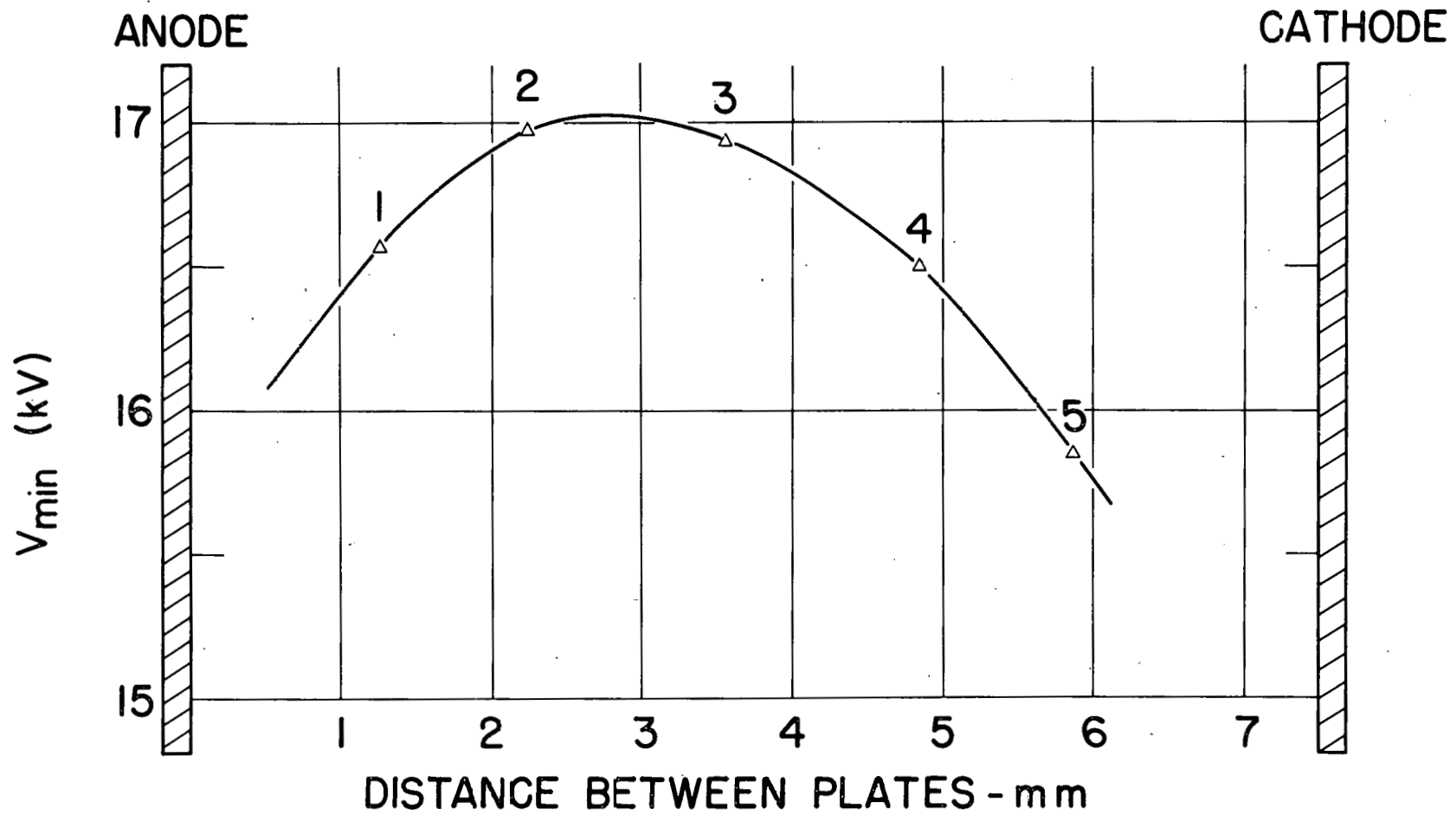


Fig. 17. Measurements of the direct voltages V_{\min} which produced the first transmission minimum along various paths between the electrodes of Cell No. 1.

VI. CALIBRATION WITH A NONUNIFORM FIELD DISTRIBUTION

A. Pulse Divider Technique

In cases where application of a direct bias voltage imposed a non-uniform field distribution, calibration was achieved by reference to pulse divider measurements as follows: The bias was adjusted until the first transmission minimum was detected. At this point, the relative field strength along the selected light path was $(E_{\min}/E_m) = \sqrt{2}$. A measured pulse voltage v_D was then applied to the biased cell; n and (I/I_m) were measured from the photomultiplier record; and (E/E_m) was determined by use of Eq. 6 or 7. Since experiments indicated that the field imposed by the pulse (duration $\approx 10 \mu s$) is uniform, the cell constant $(E_m d)$ was determined from the following equation:

$$(E_m d) = \frac{v_D}{(E/E_m) - (E_{\min}/E_m)} \quad (16)$$

Measurement of the bias voltage was not required.

Calibrations in this manner are limited only by inaccuracies in the pulse-divider measurement v_D (less than 1%) and by error in the detection of the transmission minimum (about 0.1%). The error in measurement of (I/I_m) , and thus in (E/E_m) , will be negligible if the amplitude of the applied pulse is such that $n > 10$.

Data and results from typical calibrations of Cell No. 1 by this method are given in Table 2. The calibrations were performed with the laser beam passed along the five different paths shown in Fig. 17. The cell constants determined deviated from the average by less than 0.5%.

B. Calibration from Measurements of Direct Voltages which Produce Minimum Transmission

The cell constant $(E_m d)$ was also derived from measurements (see Fig. 17) of the direct voltages which produced the first transmission minimum along paths at different distances from one of the electrodes of the cell.

Table 2. Calibrations of a Cell (No. 1) with Nonuniform Electric Field Distribution

Beam Path [Fig. 17] [mm from anode]		Method [VI-A]						Method [VI-B]			
		v_D [volts]	n	(I/I_m)	(E/E_m)	$(E_m d)$ [volts]	Δ^\dagger [%]	V_{min} [volts]	(E'/E_{min}) [from Fig. 18]	$(E_m d)$ [volts]	Δ^* [%]
1	1.26	17243	8	0.70	2.938	11314	-0.2	16567			
2	2.25	17251	8	0.69	2.937	11327	-0.04	16974			
3	3.56	17260	8	0.67	2.934	11355	+0.2	16936			
4	4.85	17273	8	0.71	2.939	11327	-0.04	$V_4 = 16506$	1.014	11512	+1.6
5	5.87	17281	8	0.70	2.938	11339	+0.1	15859			

† Deviation of calibration by Method [VI-A] from average calibration (11332 volts) by this method.

* Deviation of calibration by Method [VI-B] from calibration by Method [VI-A].

Several assumptions were made as follows: (1) that the cell constant does not vary significantly with limited changes in time, temperature, or applied voltage; and (2) that the field strength at any point between the electrodes is proportional to the applied voltage. (Experiments performed over periods of several months with several different sealed and "conditioned" cells indicated that these assumptions are reasonable.) On this basis, the field distribution imposed by application of direct voltage to Cell No. 1 was determined from the measurements of Fig. 17, in a manner similar to that used for plotting Fig. 14. The relative field strength (E/E_{\min}) as a function of distance, when the direct voltage V_4 which produced minimum transmission along path 4 (of Fig. 17) was applied to the cell, is shown by the curve in Fig. 18. The relative field strengths along paths 1, 2, 3, and 5 were deduced from the proportional changes (from V_4) in applied direct voltage required to produce the first transmission minimum along each of these paths. The relative strength (E'/E_{\min}) of the electric field which V_4 would impose if the field distribution were uniform, as determined from this curve by numerical integration, is shown by the horizontal line. The relationship between the applied terminal voltage V_4 and the voltage ($E_{\min}d$) which would produce a uniform field of intensity E_{\min} is thus:

$$V_4/(E_{\min}d) = (E'/E_{\min}) \quad , \quad (17)$$

and the cell constant may be written:

$$(E_{\min}d) = \frac{(E_{\min}d)}{\sqrt{2}} = \frac{E_{\min}}{E'} \frac{V_4}{\sqrt{2}} = \frac{V_4}{\sqrt{2} (1.014)} \quad , \quad (18)$$

with $(E_{\min}/E') = (1/1.014)$.

Calibrations obtained in this manner differed from divider calibrations by about 2%. Data and a calibration of Cell No. 1 are given in Table 2. With higher purity nitrobenzene and more accurate determination of the field distribution (from measurements of V_{\min} in the regions very close to the electrodes), we anticipate that independent calibrations to within about 1% should be feasible by this method.

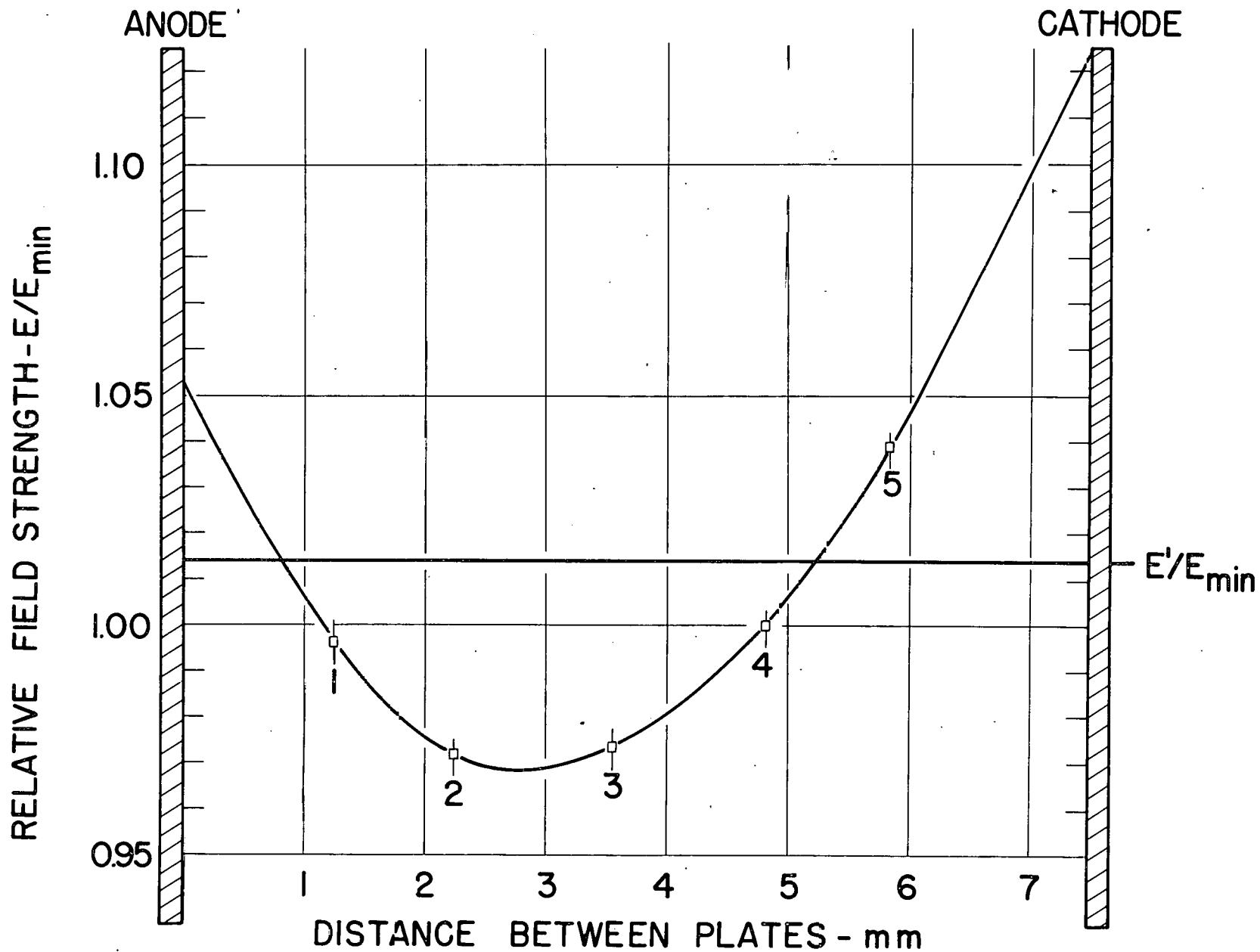


Fig. 18. Relative electric field strength (E'/E_{\min}) as a function of interelectrode distance in Cell No. 1 as deduced from the measurements of Fig. 17.

C. "Beam Expander Method"

The foregoing analysis led to the realization that $(E_m d)$ might be determined with relative ease, and perhaps greater accuracy, if the diameter of the laser beam were enlarged so that the laser radiation fell upon the entire interelectrode distance. In this case, the relative radiant flux transmitted over the interelectrode distance should be indicative of the average intensity of the nonuniform field. To test this idea, the beam expanding telescope, spatial filter, and collimating lens were attached to the laser source so that an expanded beam (diam. ≈ 50 mm) was directed between the plates of the cell as shown in Fig. 19. A mask with a rectangular slot of length slightly greater than the interelectrode distance and width 2 mm was placed in the optical path to reduce errors from field distortion over the width of the electrodes. The bias voltage which minimized the transmitted flux was then measured. The cell constant $(E_m d)$ was determined by substituting this measured bias voltage for V_{\min} in Eq. 15. Such calibrations of the two cells (Nos. 1 and 2) with 0.75 cm interelectrode distance differed from divider calibrations by less than 1%, in spite of variations as large as 10% (from the average) in local field intensities across the interelectrode distances. Typical results are compared with pulse divider calibrations (by Method VI-A) in Table 3.

After calibration, the beam expander attachment was removed from the system, and pulse measurements were made using the two calibrated cells with the beam passed along various paths between the electrodes. In each experiment direct voltage (not measured) was applied to bias the cell to the first transmission minimum. The Kerr system results v_K were then obtained by use of the following equation:

$$v_K = (E/E_m)(E_m d) - V_{\min} \quad , \quad (19)$$

where (E/E_m) was determined from the photomultiplier record as before, and V_{\min} was the bias voltage which minimized the radiant flux transmitted by the system during calibration. Deviations of v_K from v_D did not exceed 1%.

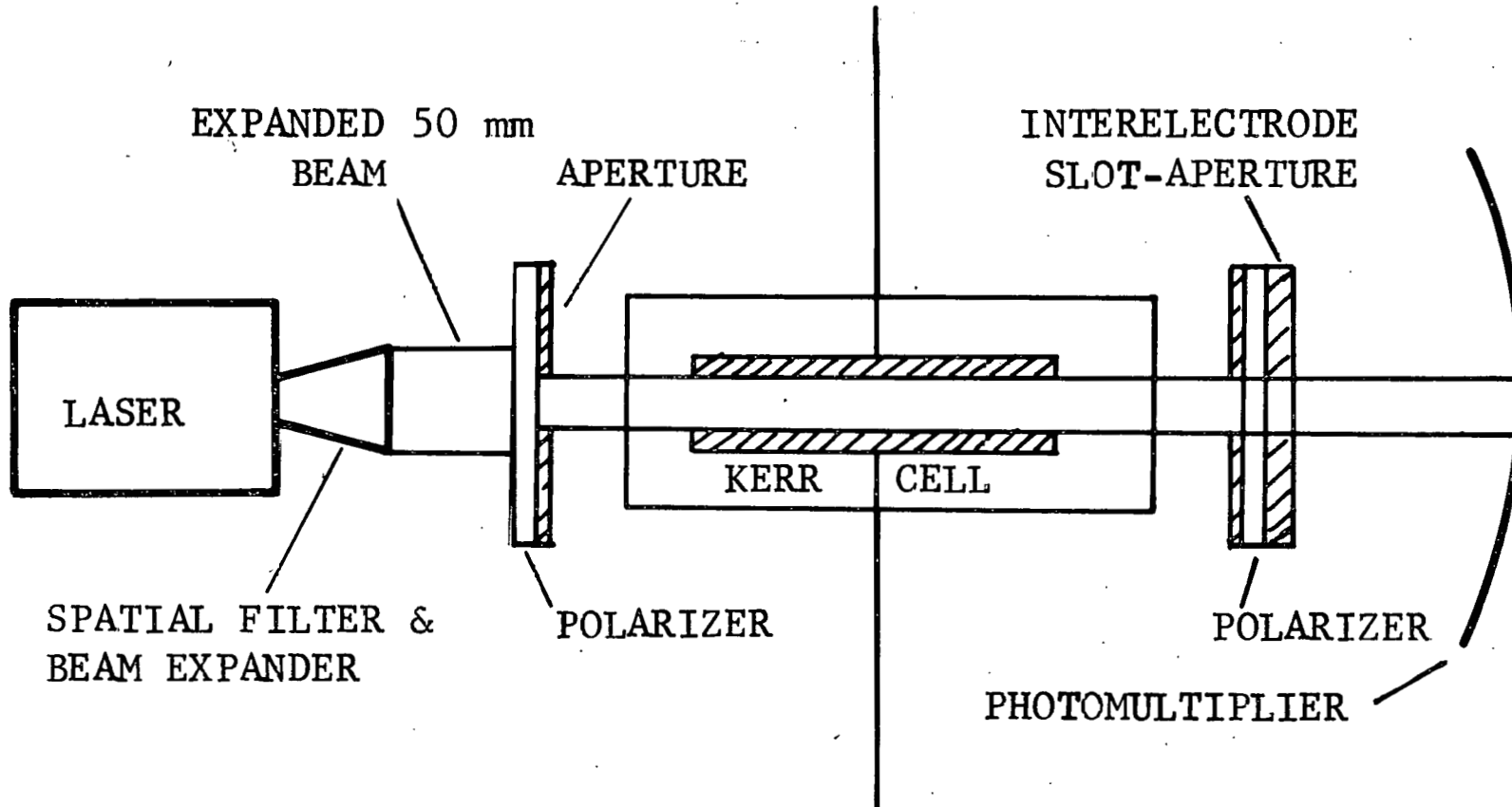


Fig. 19. SYSTEM USED FOR INDEPENDENT CALIBRATION OF
KERR SYSTEM IN PRESENCE OF FIELD DISTORTION EFFECTS

Table 3. Calibrations of Cells with Nonuniform Electric Field Distributions

	"Beam Expander Method" [VI-C]	Pulse-Divider Method [VI-A]	
	(E d) _m [volts]	(E d) _m [volts]	Δ* [%]
<u>Cell No. 1</u>	11,171	11,172	+0.01
	11,148	11,172	-0.2
	11,269	11,231	+0.3
<u>Cell No. 2</u>	9,870	9,850	+0.2
	9,890	9,935	-0.45
	9,973	9,949	-0.2

*Deviation of the cell constant (E d)_m as determined by "Beam Expander Method" [VI-C] from that determined by Pulse-Divider Method. [VI-A].

Table 4. Pulse Measurement Experiments

Table 4. Pulse Measurement Experiments						
Pulse Divider Measurements	Kerr System Results after "Beam Expander" Calibration					
v_D [volts]	Beam Path [approx.]	n	(I/I_m)	$(E_m d)$ [volts]	v_K [volts]	Δ^* [%]
<u>Cell No. 1</u>						
36,323	Near anode	21	0.05	11,171	36,417	+0.2
36,288	Center	21	0.17	11,171	36,272	-0.04
36,323	Near cathode	21	0.14	11,171	36,306	-0.05
<u>Cell No. 2</u>						
18,471	Center	10	0.86	9,890	18,446	-0.1
36,310	Near anode	25	0.29	9,950	36,307	-0.01
36,914	Center	26	0.69	9,870	36,972	+0.2
36,294	Near cathode	25	0.33	9,980	36,397	+0.3
55,088	Center	48	0.41	9,890	54,850	-0.4
73,563	Center	77	0.09	9,973	73,960	+0.5
91,979	Center	114	0.09	9,973	92,280	+0.3

*Deviation of Kerr system measurement v_K from voltage divider measurement v_D .

VII. SUMMARY AND CONCLUSION

This report summarizes progress made on the Kerr cell pulse measurements project over the past 3 years. The following are included among the principle accomplishments:

(1) Systems for purification and testing of the nitrobenzene used in our Kerr cells were developed.

(2) Methods for calibration of a Kerr system by reference to calibrated pulse divider measurements, under both uniform (Method IV-A) and nonuniform (Method VI-A), field conditions were developed. These calibrations are believed to be accurate to better than 1%.

(3) Methods for independent (without reference to pulse divider measurements), under both uniform (Method IV-B and IV-C) and nonuniform (Methods VI-B and VI-C) field conditions, were developed and evaluated.

(4) Pulse voltages as high as 100 kV were measured (simultaneously) by use of a calibrated pulse divider and a Kerr system. Several different Kerr cells were used. Results obtained after calibration by the "Beam Expander Method" [VI-C] demonstrate agreement to better than 1% between the Kerr system and the pulse divider.

With further refinements, it is anticipated that such calibrations, accurate to within $\pm 0.5\%$ will be feasible for systems capable of time-resolved measurements of pulses as high as 300 kV

VIII. FUTURE PLANS

This program will continue during the fiscal year 1969, with emphasis on the following tasks:

(1) Construction and calibration of Kerr cells with various interelectrode distances, especially of those having larger (> 1 cm) interelectrode distances required for measurement of higher voltage

pulses (> 100 kV). Investigations of the electric field distribution with various interelectrode distances will be included.

(2) Development of systems for generation and measurement (by pulse divider and Kerr system techniques) of pulse voltages as high as 300 kV.

(3) Investigation of the effect of temperature upon Kerr system calibrations.

IX. ACKNOWLEDGMENTS

The authors are grateful to Drs. F. Ralph Kotter and Harrison E. Radford for helpful discussion and suggestions, to Roger P. Chase and William A. Bagley for assistance in purification of the nitrobenzene, and to Clarence V. Kurtz and Mary C. King for assistance in preparation of this report.

X. REFERENCES

1. J. Kerr, Phil. Mag. 50, 337-348 and 446-458 (1875).
2. V. L. Pungs and H. Vogler, Phys. Zeits. 31, 485 (1930).
3. S. Namba, Rev. Sci. Instr. 27, 336 (1956).
4. S. Y. Ettinger and A. C. Venezia, Rev. Sci. Instr. 35, 221 (1963)
5. D. C. Wunsch and A. Erteza, Rev. Sci. Instr. 35, 816 (1964).
6. J. H. Park and H. N. Cones, AIEE Conf. Paper No. 57-215 (1957).
7. W. R. Fowkes and R. M. Rowe, IEEE Trans. on Instr. & Meas. IM-15, No. 4, 284-292 (December 1966).
8. A. M. Zarem, F. R. Marshall, and F. L. Poole, Elec. Eng. 68, 283 (1949).
9. N. J. Felici, Brit. J. Appl. Phys. 15, 801 (1964).

X. REFERENCES (Cont.)

10. G. Briere and N. Felici, C. R. Acad. Sc. Paris 259, 3237 (1964).
11. Calmon and Kressman, Ion Exchanges in Organic and Biochemistry, (Interscience Pub.), New York (1962), p. 201.
12. G. Jeanmaire, Revue Generale de L'Electricite 74, 3237 (1964)
14. J. H. Park and H. N. Cones, J. Res. NBS 66C, 200 (1962).

DISTRIBUTION:

F. R. Kotter, Chief
High Voltage Section
National Bureau of Standards
Washington, D. C. (25)

D. C. Wunsch
410 MacArthur
Las Cruces, New Mexico (3)

L. J. Paddison, 2400

L. J. Heilman, 7400

W. E. Boyes, 7450

S. R. Booker, 7452 (10)

W. J. Wagoner, 3413

For: DTIE (3)

M. Goldstein (1)

B. R. Allen, 3421

B. F. Hefley, 8232

C. H. Sproul, 3428-2 (10)